
Mathematics of Gravitational Lensing: Multiple Imaging and Magnification

A. O. Petters · M. C. Werner

Received: date / Accepted: date

Abstract The mathematical theory of gravitational lensing has revealed many generic and global properties. Beginning with multiple imaging, we review Morse-theoretic image counting formulas and lower bound results, and complex-algebraic upper bounds in the case of single and multiple lens planes. We discuss recent advances in the mathematics of stochastic lensing, discussing a general formula for the global expected number of minimum lensed images as well as asymptotic formulas for the probability densities of the microlensing random time delay functions, random lensing maps, and random shear, and an asymptotic expression for the global expected number of micro-minima. Multiple imaging in optical geometry and a spacetime setting are treated. We review global magnification relation results for model-dependent scenarios and cover recent developments on universal local magnification relations for higher order caustics.

Keywords Gravitational lensing · singularities

1 Introduction

1.1 Overview and Conventions

Two important anniversaries related to gravitational lensing occurred in 2009: ninety years ago the first observation of this effect was announced at a joint meeting of the Royal Society and the Royal Astronomical Society, as a successful test of Einstein's new theory of gravity; and thirty years ago Walsh, Carswell and Weyman reported the first observation of an extragalactic example of lensing. Especially since then, the subject has become a thriving research field at the interface of astronomy, theoretical physics and mathematics. Some current research highlights on astrophysical and cosmological applications of lensing have been discussed earlier in this Special Issue, as well as possible lensing tests of modified theories of gravity in the spirit of the original corroboration of General Relativity.

Of course, it has also emerged that gravitational lensing theory is a rich research area in its own right within mathematical physics. This aspect can be approached from three different directions: the widely used and astrophysically important thin-lens, weak-deflection approximation;¹ optical geometry, which considers the properties of spatial light rays, a simplification that also makes the method applicable to astrophysically relevant models; and a full general relativistic spacetime method that studies null geodesics. These approaches have proved to be mathematically quite rich, with applications of singularity theory, differential topology, Lorentzian geometry, algebraic geometry, and probability theory. In this

AOP acknowledges the partial support of NSF grant DMS-0707003.

A. O. Petters
Department of Mathematics and Department of Physics, Duke University, Durham NC 27708, USA.
E-mail: petters@math.duke.edu

M. C. Werner
Department of Mathematics, Duke University, Durham NC 27708, USA. E-mail: werner@math.duke.edu

¹ The thin-lens, weak-deflection approximation is sometimes called the *impulse approximation*.

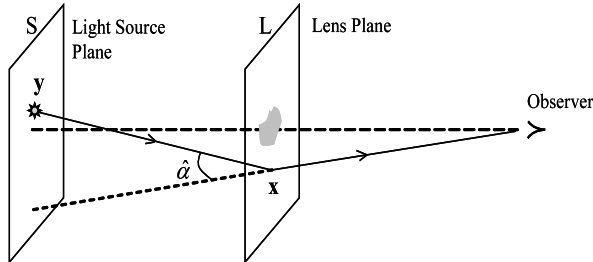


Fig. 1 A schematic of single-plane gravitational lensing. A pointlike light source is at \mathbf{y} on the light source plane S . A light ray from the source is deflected through an angle $\hat{\alpha}$ by the gravitational influence of the lens on the lens plane L .

review article, we discuss recent work in this direction on two aspects of the weak deflection limit, image counting and magnification.

One of the most basic problems in gravitational lensing is the number of images produced. Yet, already this apparently simple question turns out to be difficult. Image counting results using Morse theory and complex methods are reviewed in Section 2 for the single lens plane case, and in Section 3 for multiple lens planes. The expected number of images in stochastic lensing is discussed in Section 4, in particular for the asymptotic microlensing case of Section 5. From the point of view of optical geometry, image multiplicity is also a global effect as outlined in Section 6. Finally, conditions for the occurrence of multiple images in spacetime are summarized in Section 7. Going beyond image number, finer information on lensed images can be gained from the magnification. It turns out that image magnifications obey global magnification relations for certain lens models, and local magnification relations near singularities up to and beyond codimension three, which are universal. These results, which involve deep properties of singularities and algebraic geometry, are discussed in Sections 8, 9, and 10, respectively.

Theorem Convention: Our criteria for deciding whether a mathematical result is called a theorem will be driven by its importance in advancing our understanding of the physical and/or mathematical aspects of lensing.

Citation Conventions: The first time a result from a paper is mentioned, the name(s) of the author(s) are stated next to the bibliographic reference. Thereafter, citations of the same result have the bibliographic reference without the names. The authors of this article are cited as AOP for Petters and MCW for Werner.

Miscellaneous Conventions: All light sources are treated as point-like. The symbol \equiv indicates that a definition is given. Physical quantities are given in appropriate dimensionless forms.

1.2 Notation for Some Basic Weak Deflection Lensing Concepts

Denote the dimensionless potential of a gravitational lens by ψ . The (dimensionless) surface mass density κ and magnitude Γ of shear are:

$$\kappa(\mathbf{x}) = \frac{1}{2} \nabla^2 \psi(\mathbf{x}), \quad \Gamma^2(\mathbf{x}) = \frac{1}{4} (\psi_{uu}(\mathbf{x}) - \psi_{vv}(\mathbf{x}))^2 + \psi_{uv}^2(\mathbf{x}),$$

where $\mathbf{x} = (u, v)$. Note that \mathbf{x} is dimensionless, i.e., $\mathbf{x} = \mathbf{r}/d_L$ with \mathbf{r} the physical impact vector in the plane of the physical lens at angular diameter distance d_L ; see Figure 1. Since $d_L \gg |\mathbf{r}|$, we can treat \mathbf{x} as an angular vector. A *singularity* of ψ is a point $\mathbf{a} \in \mathbb{R}^2$ such that either $\psi(\mathbf{x}) \rightarrow -\infty$ or $\nabla^2 \psi(\mathbf{x}) \rightarrow \infty$ as $\mathbf{x} \rightarrow \mathbf{a}$. In particular, an *infinite singularity* of ψ is a singularity \mathbf{a} for which $\psi(\mathbf{x}) \rightarrow -\infty$ as $\mathbf{x} \rightarrow \mathbf{a}$. We shall call ψ *nonsingular* if it has no singularities. The potential ψ is assumed to be smooth (C^∞) everywhere on \mathbb{R}^2 , except on the set A of singularities of ψ .

Let $T_{\mathbf{y}} : L \rightarrow \mathbb{R}$ be the (dimensionless) single-plane time delay function induced by a lens potential ψ , where $L = \mathbb{R}^2 - A$ with A the set of singularities of ψ :

$$T_{\mathbf{y}}(\mathbf{x}) = \frac{|\mathbf{x} - \mathbf{y}|^2}{2} - \psi(\mathbf{x}).$$

Unless stated to the contrary, we assume that A is a finite set. The point \mathbf{y} lies in the light source plane $S = \mathbb{R}^2$; see Figure 1. The light source plane S is the set of all “angular” source positions $\mathbf{y} = \mathbf{s}/d_S$,

where \mathbf{s} is a physical (linear) source position in the Euclidean plane at angular diameter distance d_S and orthogonal to the line of sight.

By Fermat's principle [72,64], the light rays connecting \mathbf{y} to the observer are given by the critical points of $T_{\mathbf{y}}$, i.e., solutions $\mathbf{x} \in L$ of

$$\mathbf{0} = \nabla T_{\mathbf{y}}(\mathbf{x}) = -\mathbf{y} + \mathbf{x} - \nabla\psi(\mathbf{x}),$$

where the gradients are with respect to the rectangular coordinates $\mathbf{x} = (u, v)$. The above equation determines the single-plane lensing map corresponding to $T_{\mathbf{y}} : L \rightarrow \mathbb{R}$, namely, the transformation $\boldsymbol{\eta} : L \rightarrow S$ defined by:

$$\boldsymbol{\eta}(\mathbf{x}) = \mathbf{x} - \nabla\psi(\mathbf{x}).$$

The *lensed images* of a light source at \mathbf{y} are the elements of $\boldsymbol{\eta}^{-1}(\mathbf{y})$ or, equivalently, the critical points of $T_{\mathbf{y}}$. Through this correspondence, we speak of minimum, saddle, and maximum lensed images.

Example (Microlensing): We define microlensing generally as due to a lens consisting of g stars with masses m_1, \dots, m_g at respective positions $\boldsymbol{\xi}_1, \dots, \boldsymbol{\xi}_g$, continuous matter with constant density $\kappa_c \geq 0$, and an external shear $\gamma \geq 0$. The lens potential of microlensing is then given by:

$$\psi_g(\mathbf{x}) = \frac{\kappa_c}{2}|\mathbf{x}|^2 - \frac{\gamma}{2}(u^2 - v^2) + \sum_{j=1}^g m_j \log |\mathbf{x} - \boldsymbol{\xi}_j|,$$

where $\mathbf{x} = (u, v)$. The induced time delay function $T_{g,\mathbf{y}}$ at \mathbf{y} is

$$T_{g,\mathbf{y}}(\mathbf{x}) = \frac{1}{2}|\mathbf{x} - \mathbf{y}|^2 - \frac{\kappa_c}{2}|\mathbf{x}|^2 + \frac{\gamma}{2}(u^2 - v^2) - \sum_{j=1}^g m_j \log |\mathbf{x} - \boldsymbol{\xi}_j|$$

and the corresponding lensing map $\boldsymbol{\eta}_g$ is

$$\boldsymbol{\eta}_g(\mathbf{x}) = ((1 - \kappa_c + \gamma)u, (1 - \kappa_c - \gamma)v) - \sum_{j=1}^g m_j \frac{\mathbf{x} - \boldsymbol{\xi}_j}{|\mathbf{x} - \boldsymbol{\xi}_j|^2}.$$

We shall refer to the lensed images in microlensing as *micro-images* and may even speak of *micro-minima* to designate minimum images in this context.

The (*absolute*) *magnification* of a lensed image is physically the ratio of the flux of the image to the flux of the light source, which is given mathematically by (e.g., [64], p. 85):

$$\text{Mag}(\mathbf{x}; \mathbf{y}) = \frac{1}{|\det[\text{Jac } \boldsymbol{\eta}](\mathbf{x})|}, \quad \boldsymbol{\eta}(\mathbf{x}) = \mathbf{y}.$$

Note that $\det[\text{Jac } \boldsymbol{\eta}](\mathbf{x}) = \det[\text{Hess } T_{\mathbf{y}}](\mathbf{x}) = (1 - \kappa(\mathbf{x}))^2 - \Gamma^2(\mathbf{x})$. The *signed magnification* of lensed image \mathbf{x}_i of \mathbf{y} is defined by:

$$\mu_i = (-1)^{\text{Ind}(\mathbf{x}_i)} \text{Mag}(\mathbf{x}_i; \mathbf{y}), \quad \boldsymbol{\eta}(\mathbf{x}_i) = \mathbf{y}.$$

Here $\text{Ind}(\mathbf{x}_i)$ is the Morse index of \mathbf{x}_i , i.e., the number of negative eigenvalues of $(\text{Hess } T_{\mathbf{y}})(\mathbf{x}_i)$, which is 0, 1, and 2 for a minimum, saddle, and maximum, respectively.

The set $\text{Crit}(\boldsymbol{\eta})$ of *critical points* of $\boldsymbol{\eta}$ is the set of all (formally) infinitely magnified lensed images for all light source positions in S , which consists of all $\mathbf{x} \in L$ where $\det[\text{Jac } \boldsymbol{\eta}](\mathbf{x}) = 0$. When $\text{Crit}(\boldsymbol{\eta})$ consists of curves, we shall speak of the *critical curves* of $\boldsymbol{\eta}$. The set of *caustics* of $\boldsymbol{\eta}$ is $\text{Caustic}(\boldsymbol{\eta}) = \boldsymbol{\eta}(\text{Crit}(\boldsymbol{\eta})) \subset S$, which is the set of all light source positions from which there is at least one infinitely magnified lensed image. For physically relevant settings, the set $\text{Crit}(\boldsymbol{\eta})$ is bounded, which yields that $\text{Crit}(\boldsymbol{\eta})$ and $\text{Caustic}(\boldsymbol{\eta})$ are compact ([64], p. 293).

The single-plane time delay function $T_{\mathbf{y}}$ is said to be *subcritical at infinity* if for each non-caustic point \mathbf{y} and $|\mathbf{x}|$ sufficiently large, the eigenvalues $\lambda_1(\mathbf{x}; \mathbf{y})$ and $\lambda_2(\mathbf{x}; \mathbf{y})$ of $\text{Hess } T_{\mathbf{y}}(\mathbf{x})$ are positive. This means that

$$\lambda_1(\mathbf{x}; \mathbf{y}) = 1 - \kappa(\mathbf{x}) + \Gamma(\mathbf{x}) > 0, \quad \lambda_2(\mathbf{x}; \mathbf{y}) = 1 - \kappa(\mathbf{x}) - \Gamma(\mathbf{x}) > 0. \quad (1)$$

Condition (1) implies:

$$0 \leq \kappa(\mathbf{x}) < 1, \quad 0 \leq \Gamma(\mathbf{x}) < 1.$$

In addition, the time delay surface (graph) of $T_{\mathbf{y}}$ then has positive Gauss curvature for $|\mathbf{x}|$ sufficiently large. When $T_{\mathbf{y}}$ is subcritical at infinity and $T_{\mathbf{y}}(\mathbf{x}) \rightarrow \infty$ as $|\mathbf{x}| \rightarrow \infty$, we call $T_{\mathbf{y}}$ *isolated*.

Given that the lensed images of a light source at \mathbf{y} are in 1-1 correspondence with the critical points of $T_{\mathbf{y}}$, we shall characterize each lensed image as either a minimum, saddle, or maximum.

Notation:

1. N = total number of images.
2. N_{\min} = number of minimum images.
3. N_{sad} = number of saddle images.
4. N_{\max} = number of maximum images.
5. $N_+ = N_{\min} + N_{\max}$ = number of positive parity images.

2 Multiple Imaging in Single-Plane Lensing

2.1 Image Counting Formulas and Lower Bounds: Single Plane Lensing

Einstein determined in 1912 [71] that a lens consisting of a single star will produce *two* images of a background star that is not on a caustic. Two stars on the same lens plane can produce either *three* or *five* images for light sources off a caustic, a result found in 1986 by Schneider and Weiss [73]. The method in [73], however, involved lengthy calculations that directly solved the lens equation for the images, an approach that would be impossible to carry over to any finite number of stars or more general mass distributions.

In 1991, AOP [61] approached the image counting problem by employing Morse theory under boundary conditions and generic properties of time delay functions to obtain a general theorem yielding counting formulas and lower bounds for the number of images. The Morse theoretic approach is particularly powerful because it gives specific counting information about the number of images of different types and extends naturally to k -lens planes and a general spacetime setting. For simplicity, we state the results in [61] only for generic subcritical lensing (see [64, Chap. 11] for more):

Theorem 1 [61] (**Single-Plane Image Counting Formulas and Lower Bounds**) *Let $T_{\mathbf{y}} : L \rightarrow \mathbb{R}$ be a single-plane time delay function induced by a lens potential ψ with $g \geq 0$ singularities, all of which are infinite singularities. Suppose that \mathbf{y} is not on a caustic and $T_{\mathbf{y}}$ is isolated. Then for a generic² $T_{\mathbf{y}}$ the number of lensed images obeys:*

1. $N = 2N_+ + g - 1 = 2N_{\text{sad}} - g + 1$, $N_+ = N_{\text{sad}} - g + 1$.
2. $N \geq g + 1$, $N_{\min} \geq 1$, $N_{\text{sad}} \geq N_{\max} + g$.
3. *If the corresponding lensing map is locally stable³ with $\text{Crit}(\boldsymbol{\eta})$ bounded, then for sufficiently large $|\mathbf{y}|$ the lower bounds on the number of images are attained:
 $N = g + 1$, $N_{\min} = 1$, $N_{\max} = 0$, and $N_{\text{sad}} = g$.*

As long as the hypotheses of Theorem 1 hold, the image counting information is independent of the choice of gravitational lens model. The topological nature of the counting formulas and lower bounds give them wide applicability. Part 1 of Theorem 1 states that the number of images has parity (even-ness or odd-ness) opposite to the number of singularities, part 2 gives lower bounds—e.g., there are at least $g + 1$ images and at least g saddle images, and part 3 implies that the lower bounds in Part 2 are actually the smallest number of images that are achievable.

Application to microlensing: Theorem 1 applies to subcritical microlensing, i.e., lensing due to g point masses with continuous matter κ_c and shear γ satisfying $1 - \kappa_c + \gamma > 0$ and $1 - \kappa_c - \gamma > 0$. There is an even number of images if and only if the number of stars is odd. Also, since there is no maximum images, we have

$$N_{\min} = N_{\text{sad}} - g + 1.$$

² Theorem 1 holds either for $T_{\mathbf{y}}$ or almost all sufficiently small linear perturbations of $T_{\mathbf{y}}$, i.e., the functions $T_{\mathbf{y}}(\mathbf{x}) + \mathbf{p} \cdot \mathbf{x}$ for every $\mathbf{p} \in \mathbb{R}^2$, except in a set of measure zero, with $|\mathbf{p}|$ sufficiently small [64, p. 421].

³ Local stability is equivalent to the set of critical points of $\boldsymbol{\eta}$ consisting only of folds and cusps [64, p. 294].

This is a useful formula for checking whether images are overlooked by in microlensing simulations. Consult [64, Chap. 11] for a detailed discussion, where the cases $1 - \kappa_c + \gamma > 0$ and $1 - \kappa_c + \gamma < 0$ (strong shear lensing) and $1 - \kappa_c + \gamma < 0$ and $1 - \kappa_c + \gamma < 0$ (supercritical lensing) are also treated.

In the situation of a nonsingular lens, the following corollary of Theorem 1(1) recovers (by setting $g = 0$) the single-plane Odd Number Image Theorem found in 1981 by Burke [16], who proved the result using a different approach, namely, the Poincaré-Hopf index theorem.

Corollary 1 [16] (Single-Plane Odd Number Image Theorem) *For a non-caustic point \mathbf{y} , let $T_{\mathbf{y}}$ be a single-plane isolated time delay function induced by a nonsingular gravitational lens potential. Then the total number of images is odd:*

$$N = 2N_+ - 1 = 2N_{\text{sad}} + 1.$$

Nonsingular lensing is typically due to modeling galaxies as smooth on a macro scale. Though the predicted number of images is odd, typically an even number of images is observed. The reason is that maximum images are angularly located where the surface mass density of the lens is supercritical (core of galaxies), which causes them to become significantly demagnified (e.g., [51], [64, p. 470]).

We saw from Theorem 1(2) that if an isolated lens has at least one singularity ($g \geq 1$), which can be a point mass, singular isothermal sphere, etc., then the lens can produce multiple images. Namely, there is a point in the light source plane from which a light source has more than one lensed image, $N > 1$. How about multiple imaging due to an isolated nonsingular lens? The following necessary and sufficient condition for multiple imaging by such lenses was established in 1986 by Subramanian and Cowling [78]:

Theorem 2 [78] (Criterion for Multiple Images: Single-Plane Nonsingular Case) *For a non-caustic point \mathbf{y} , let $T_{\mathbf{y}}$ be a single-plane isolated time delay function induced by a nonsingular gravitational lens potential. Then:*

1. $N \geq 3$ if and only if there is a point \mathbf{x}_0 in the lens plane L such that $\det[\text{Hess } T_{\mathbf{y}}](\mathbf{x}_0) < 0$.
2. If there is a point $\mathbf{x}_0 \in L$ where the surface mass density is supercritical, $\kappa(\mathbf{x}_0) > 1$, then a light source at $\mathbf{y}_0 = \boldsymbol{\eta}(\mathbf{x}_0)$ will have multiple images, $N \geq 3$.

We prove Theorem 2 to illustrate how some of the previous counting results and ideas are used theoretically.

Proof (1) If $N > 1$, then Corollary 1(1) yields $N = 2N_{\text{sad}} + 1 \geq 3$, so $N_{\text{sad}} \geq 1$. Because there is at least one saddle image, say, \mathbf{x}_{sad} , the point $\mathbf{x}_{\text{sad}} \in L$ satisfies $\det[\text{Hess } T_{\mathbf{y}}](\mathbf{x}_{\text{sad}}) < 0$. Conversely, if there is a point $\mathbf{x}_0 \in L$ such that $\det[\text{Hess } T_{\mathbf{y}}](\mathbf{x}_0) < 0$, then a light source at $\mathbf{y}_0 = \boldsymbol{\eta}(\mathbf{x}_0)$ has at least one saddle image. Since $N_{\text{sad}} \geq 1$, $N_{\text{min}} \geq 1$, and the number of images is odd, we have $N \geq 3$.

(2) If $\kappa(\mathbf{x}_0) > 1$, then image \mathbf{x}_0 cannot be a minimum since minima are located where the surface mass density is subcritical (e.g., [64, p. 423]). Then \mathbf{x}_0 is either a saddle or maximum. For \mathbf{x}_0 a maximum, Theorem 1(2) with $g = 0$ (nonsingular case) yields $N_{\text{sad}} \geq N_{\text{max}} \geq 1$, which yields $N \geq 3$ (since $N_{\text{min}} \geq 1$). For \mathbf{x}_0 a saddle, we get $N \geq 1$ because there is also at least one minimum and the number of images must be odd. \square

The sufficient condition $\kappa(\mathbf{x}_0) > 1$ for multiple images of a source at $\mathbf{y}_0 = \boldsymbol{\eta}(\mathbf{x}_0)$ is not also a necessary condition. A perturbed Plummer lens has the following respective potential and surface mass density:

$$\psi(\mathbf{x}) = \frac{\kappa_0}{2} \log(1 + |\mathbf{x}|^2) - \frac{\gamma}{2}(u^2 - v^2), \quad \kappa(\mathbf{x}) = \frac{\kappa_0}{(1 + |\mathbf{x}|^2)^2},$$

where $\gamma > 0$ is the external shear and $\mathbf{x} = (u, v)$. This lens is subcritical everywhere for $0 < \kappa_0 < 1$, but can still produce multiple images (e.g., [64, p. 429]).

Multiple imaging is also discussed in Section 6 from the optical geometry point of view, and for nonsingular lenses in a spacetime context in Section 7.

2.2 Maximum Number of Images: Single Plane Lensing

A natural next question is to determine the maximum attainable number of images due to g stars. Using a trick with complex quantities, Witt [82] showed in 1990 that g point masses will generate at most $g^2 + 1$ images. Since it was unclear how to extend the trick in [82] to multiplane lensing, AOP [63] gave in 1997 an alternative proof of the upper bound using resultants, an approach generalizable to multiple lens planes (see Section 3.2).

Combining the above upper bound result with Theorem 1(2), the number of images is bounded as follows:

$$g + 1 \leq N \leq g^2 + 1. \quad (2)$$

For two point masses $g = 2$, equation (2) yields $N = 3, 4$ or 5 . However, we cannot have $N = 4$ since by Theorem 1(1) an even number of stars has to produce an odd number of images. Hence, $N = 3$ or 5 , which recovers the result in [73].

It remained unclear whether the quadratic upper bound of $g^2 + 1$ in (2) can be attained. In 1997, Mao, AOP, and Witt [46] conjectured that the maximum number of lensed images should be linear in g . They also constructed a lens system consisting of g point masses of equal mass $1/g$ on the vertices of a regular polygon and showed that this symmetrical system produces a maximum number of $3g + 1$ images. The latter is a linear lower bound on the maximum number of images for g point masses. Rhie [70] showed in 2003 that by putting a mass $m_\epsilon > 0$ at the center of the regular polygon, but with equal masses $1/(g - 1)$ on its vertices, a total of $5g - 5$ images can be achieved for sufficiently small masses. Using a modification of the method in [46], Bayer and Dyer [13] gave in 2007 a much simpler proof of the result in [70] and improved our understanding of the result by determining an upper bound m_\star of the central mass such that the maximum number $5g - 5$ of images is attained for all $m_\epsilon < m_\star$. The conjecture was finally settled in 2006 when Khavinson and Neumann [42] employed complex rational harmonic functions to show that the total number of images is at most $5g - 5$. The results are summarized below:

Theorem 3 (Maximum Number of Images: Single-Plane Case) *For $g \geq 2$ point masses on a lens plane and a light source not on a caustic, the number of images satisfies:*

1. [42] $N \leq 5g - 5$.
2. The upper bound $5g - 5$ is attainable for:
 - (a) [46] $g = 3$ if the point masses have equal mass $1/g$ and lie on the vertices of an equilateral triangle centered at the origin and inscribed in a circle of radius r bounded above as follows:

$$r < r_{\text{cr}} \equiv \left[\left(\frac{g-2}{g} \right)^{g-2/2} - \left(\frac{g-2}{g} \right)^{g/2} \right]^{g-2/g}.$$

- (b) [70, 13] $g \geq 4$ if $g - 1$ of the point masses have equal mass $1/(g - 1)$ and lie on the vertices of a regular polygon centered at the origin and inscribed in a circle of radius $r < r_{\text{cr}}$, and a point mass of m_ϵ is at the center of the polygon with mass upper bound given by:

$$0 < m_\epsilon < m_\star \equiv r^2 \left(\frac{g+5}{g-1} \right) - \frac{r^6}{1+r^6}.$$

We now have the following sharp (i.e., attainable) bounds on the total number of images due to point masses:

$$g + 1 \leq N \leq 5g - 5, \quad g \geq 2. \quad (3)$$

Remark: For lensing by a general matter distribution, there is no overarching maximum number of images because a mass clump can always be added to a lens to create more images.

3 Multiple Imaging in Multiplane Lensing

To set up the image counting results for multiple lens planes, we review some of the notation and concepts needed. Consult [64, Chap. 6] for more details.

Let L_i be the i th lens plane counting from observer to the light source plane and set $\mathbf{X} = (\mathbf{x}_1, \dots, \mathbf{x}_k) \in L_1 \times \dots \times L_k$; see Figure 2. Denote the gravitational lens potential on L_i by ψ_i , where $i = 1, \dots, k$, and

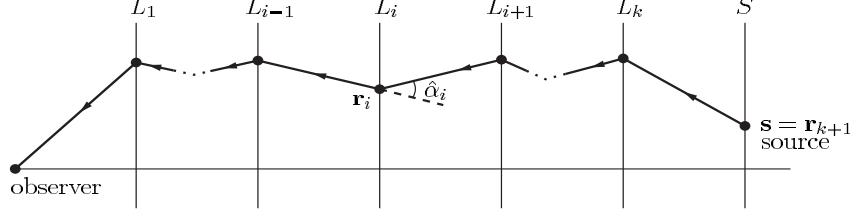


Fig. 2 A schematic of k -plane gravitational lensing. The action of the lensing map is captured by tracing light rays backwards from a subset P of L_1 to the light source plane S . Credits: After [64, p. 199].

the light source plane by $S = \mathbb{R}^2$ with its elements $\mathbf{y} \in S$. Let $T_{\mathbf{y}}^{(k)} : L_1 \times \cdots \times L_k \rightarrow \mathbb{R}$, be the k -plane time delay function induced by the potentials ψ_i and denote the associated k -plane lensing map by $\boldsymbol{\eta}^{(k)} : P \rightarrow S$. Here $P = \mathbb{R}^2 - B \subseteq L_1$, where B is the set of light path obstruction points. Note that for single-plane lensing $P = L_1 = L$ and $B = A$ (set of singularities of the potential $\psi_1 = \psi$).

The set $\text{Crit}(\boldsymbol{\eta}^{(k)})$ of *critical points* of $\boldsymbol{\eta}^{(k)}$ is the locus of all infinitely magnified lensed images for all light source positions in S , while the set of *caustics* of $\boldsymbol{\eta}^{(k)}$ is $\text{Caustic}(\boldsymbol{\eta}^{(k)}) = \boldsymbol{\eta}^{(k)}[\text{Crit}(\boldsymbol{\eta}^{(k)})] \subset S$, i.e., the set of all light source positions from which there is at least one infinitely magnified lensed image. When $\text{Crit}(\boldsymbol{\eta}^{(k)})$ is bounded, then both $\text{Crit}(\boldsymbol{\eta}^{(k)})$ and $\text{Caustic}(\boldsymbol{\eta}^{(k)})$ are compact [64, p. 293].

The k -plane time delay function $T_{\mathbf{y}}^{(k)}$ is called *subcritical at infinity* if for each non-caustic point \mathbf{y} and $|\mathbf{X}|$ sufficiently large, the eigenvalues of $\text{Hess } T_{\mathbf{y}}^{(k)}(\mathbf{X})$ are positive, i.e., the time delay surface has positive Gauss-Kronecker curvature for $|\mathbf{X}|$ sufficiently large. If $T_{\mathbf{y}}^{(k)}$ is subcritical at infinity and $T_{\mathbf{y}}^{(k)}(\mathbf{X}) \rightarrow \infty$ as $|\mathbf{X}| \rightarrow \infty$, then $T_{\mathbf{y}}^{(k)}$ is called *isolated*.

By Fermat's principle, the critical points of $T_{\mathbf{y}}^{(k)}$ determine the lensed images of a source at \mathbf{y} (e.g., [64], Chaps. 3,6), so the lensed images are then identified as generalized saddles of index i , where $i = 0, 1, \dots, 2k$.

Notation:

1. N_i = number of images of index i . Here N_0 and N_{2k} are, resp., the number of minima and maxima.
2. $N_+ = \sum_{i(\text{even})} N_i$ = number of even index images.
3. $N_- = \sum_{i(\text{odd})} N_i$ = number of odd index images.
4. $N = N_+ + N_-$ = total number of images.

3.1 Counting Formulas and Lower Bounds in Multiplane Lensing

In 1991, AOP [61] extended to k -lens planes the image counting results of Theorem 1, including the Odd Number Image Theorem. All the results are topological in nature, which give them wide applicability. As before, we state the results only for the subcritical case (see [64, Chap.12] for more):

Theorem 4 [61] (**Multiplane Counting Formulas and Lower Bounds**) *Let $T_{\mathbf{y}}^{(k)} : L_1 \times \cdots \times L_k \rightarrow \mathbb{R}$ be a k -plane time delay function induced by lens potentials ψ_1, \dots, ψ_k , where each ψ_i has g_i singularities, each of which is an infinite singularity. Assume that \mathbf{y} is a non-caustic point and $T_{\mathbf{y}}^{(k)}$ is isolated. Then for a generic^A $T_{\mathbf{y}}^{(k)}$ the number of lensed images satisfies:*

1. $N = 2N_+ - \prod_{i=1}^k (1 - g_i) = 2N_- + \prod_{i=1}^k (1 - g_i), \quad N_+ = N_- + \prod_{i=1}^k (1 - g_i).$
2. $N \geq \prod_{i=1}^k (1 + g_i).$
3. $N_0 \geq 1, \quad N_j \geq \sum_{1 \leq \ell_1 < \cdots < \ell_j \leq k} g_{\ell_1} \cdots g_{\ell_j} \text{ for } 1 \leq j \leq k, \quad \text{and } N_j \geq 0 \text{ for } k+1 \leq j \leq 2k-1.$

^A Theorem holds either for $T_{\mathbf{y}}^{(k)}$ or $T_{\mathbf{y}}^{(k)}(\mathbf{X}) + \hat{\mathbf{p}} \cdot \mathbf{X}$, for sufficiently small $\hat{\mathbf{p}} \in \mathbb{R}^{2k}$, except in a set of measure zero [64, pp. 452-455].

4. If the corresponding lensing map $\boldsymbol{\eta}^{(k)}$ is locally stable and $\text{Crit}(\boldsymbol{\eta}^{(k)})$ is bounded, then for sufficiently large $|\mathbf{y}|$ the above lower bounds on the number of images of different types are attained:

$$N = \prod_{i=1}^k (1 + g_i), \quad N_0 = 1, \quad N_j = \sum_{1 \leq \ell_1 < \dots < \ell_j \leq k} g_{\ell_1} \cdots g_{\ell_j} \quad \text{for } 1 \leq j \leq k,$$

and $N_j = 0$ for $k + 1 \leq j \leq 2k - 1$.

Corollary 2 (Multiplane Odd Number Image Theorem) For a non-caustic point \mathbf{y} , let $T_{\mathbf{y}}^{(k)}$ be a isolated k -plane time delay function induced by nonsingular gravitational lens potentials. Then:

$$N = 2N_+ - 1 = 2N_- + 1.$$

3.2 An Upper Bound on the Number of Images

A natural question is whether there are multiplane lensing bounds on the number of images analogous to the single-plane ones in (2) or (3). The following 1997 theorem of AOP [63] is what is known so far:

Theorem 5 [63] (Multiplane Upper Bound) Let \mathbf{y} be a non-caustic point. Then the total number of images due to gravitational lensing by g point masses on g lens planes with one point mass on each lens plane is bounded as follows:

$$2^g \leq N \leq 2 \left(2^{2(g-1)} - 1 \right), \quad g \geq 2. \quad (4)$$

By Theorem 4(1,4), the lower bound of 2^g is sharp and the total number of images is always even. Theorem 5 was proven using the theory of resultants.

4 General Stochastic Lensing: The Expected Number of Minimum Images

Stochastic lensing occurs when a component of a systems is random, typically, the lens. This relates to the broader study of random functions, a subject that has been explored in mathematics primarily for Gaussian random fields (e.g., Adler and Taylor [5], Azais and Wschebor [12], Forrester and Honner [25], Li and Wei [44], Shub and Smale [76], Sodin and Tsirelson [77], and references therein). However, in gravitational lensing most of the realistic lensing scenarios produce non-Gaussian random fields that have not been previously considered (e.g., see Theorem 7 below). Therefore, a new mathematical framework needs to be developed for the study of stochastic lensing.

A natural first step in stochastic lensing is to study the expectation of the random number of lensed images. We shall present some recent rigorous mathematical work in that direction.

The expectation of $N_+(D, \mathbf{y})$, the number of positive parity lensed images inside a closed disk D of a light source at position \mathbf{y} , is given by the following Kac-Rice type formula (see [66]):

$$E[N_+(D, \mathbf{y})] = \int_D E \left[((1 - \kappa(\mathbf{x}))^2 - \Gamma^2(\mathbf{x})) \mathbf{1}_{\mathcal{G}_A}(\mathbf{x}) \mid \boldsymbol{\eta}(\mathbf{x}) = \mathbf{y} \right] f_{\boldsymbol{\eta}(\mathbf{x})}(\mathbf{y}) \, d\mathbf{x}, \quad (5)$$

for almost all \mathbf{y} . Here, $\mathbf{1}_{\mathcal{G}_A}$ is the indicator function on $\mathcal{G}_A = \{\nu \in \mathbb{R}^2 : G(\nu) \in (0, \infty)\}$, where $G(\mathbf{x}) = \det[\text{Jac } \boldsymbol{\eta}](\mathbf{x})$, and $f_{\boldsymbol{\eta}(\mathbf{x})}$ is the probability density function (p.d.f.) of the lensing map at \mathbf{x} .

This formula holds for a fixed light source position. Unfortunately, this position is unknown in most lensing observations. Therefore, a physically relevant extension of (5) is to view the light source position as a random variable whose probability density function is compactly supported over a subset of the light source plane having positive measure. This result can be further generalized to the entire light source plane. To do so, a countable compact covering $\{\mathfrak{S}\}$ of light source plane is considered, with each set \mathfrak{S} in the family having the same positive area. A corresponding family $\{Y_{\mathfrak{S}}\}$ of random light source positions Y is constructed, with each Y uniformly distributed over a set \mathfrak{S} . The *global expectation* of the number of positive parity lensed images, denoted by $\bar{E}[N_+(D, Y; \mathfrak{S})]_{\{\mathfrak{S}\}}$, is then defined as the average of $E[N_+(D, y)]$ over the family $\{Y_{\mathfrak{S}}\}$ (equivalently, over the family $\{\mathfrak{S}\}$). This notion was introduced in [66].

AOP, Rider, and Teguiá 2009 [66] determined a general formula for the global expected number of positive parity images:

Theorem 6 [66] (**Global Expected Number of Positive Parity Images**) *The global expectation of the number of positive parity lensed images in D is given by:*

$$\widehat{E}[N_+(D, Y; \mathfrak{S})]_{\{\mathfrak{S}\}} = \frac{1}{|\mathfrak{S}_0|} \int_D E[\det[\text{Jac } \boldsymbol{\eta}](\mathbf{x}) \mathbf{1}_{\mathcal{G}_A}(\mathbf{x})] d\mathbf{x}, \quad (6)$$

where $|\mathfrak{S}_0| = \text{area}(\mathfrak{S})$.

The importance of Theorem 6 is its applicability to a wide range of lensing scenarios, with few assumptions on the distribution of the random gravitational field within each scenario. Below we will discuss an application of this theorem to image counting in microlensing.

5 Stochastic Microlensing: Asymptotics

The mathematical analysis of the p.d.f.s and expectations in microlensing is very difficult. An asymptotic approach is a natural first step that will be important for understanding first order terms and how deviations from them occur at subsequent orders. For example, we shall see that, though the lensing map of microlensing is a bivariate Gaussian at first order, the mapping deviates from Gaussianity at the next orders. The p.d.f.s of the time delay function and shear will also be seen to be non-Gaussian. Unfortunately, this means that most of the technology already developed in the mathematical theory of random fields will not be applicable directly to stochastic lensing.

5.1 Notation

The stochastic microlensing scenario we shall discuss is one with uniformly distributed random star positions. Recall from the Introduction that the potential is given by

$$\psi_g(\mathbf{x}) = \frac{\kappa_c}{2} |\mathbf{x}|^2 - \frac{\gamma}{2} (u^2 - v^2) + \sum_{j=1}^g m_j \log |\mathbf{x} - \boldsymbol{\xi}_j|,$$

where $\mathbf{x} = (u, v)$, the time delay function at \mathbf{y} by

$$T_{g,\mathbf{y}}(\mathbf{x}) = d_1(\mathbf{x}; \mathbf{y}) - \sum_{j=1}^g m_j \log |\mathbf{x} - \boldsymbol{\xi}_j|,$$

where $d_1(\mathbf{x}; \mathbf{y}) = \frac{1}{2} |\mathbf{x} - \mathbf{y}|^2 - \frac{\kappa_c}{2} |\mathbf{x}|^2 + \frac{\gamma}{2} (u^2 - v^2)$, and the components of the lensing map $\boldsymbol{\eta}_g = (\boldsymbol{\eta}_{1,g}, \boldsymbol{\eta}_{2,g})$ by:

$$\begin{aligned} \boldsymbol{\eta}_{1,g}(\mathbf{x}) &= (1 - \kappa_c + \gamma)u - \sum_{j=1}^g m \frac{U_j - u}{(U_j - u)^2 + (V_j - v)^2}, \\ \boldsymbol{\eta}_{2,g}(\mathbf{x}) &= (1 - \kappa_c - \gamma)v - \sum_{j=1}^g m \frac{V_j - v}{(U_j - u)^2 + (V_j - v)^2}, \end{aligned}$$

where $\boldsymbol{\xi}_j = (U_j, V_j)$.

Notation and Assumptions:

1. Equal masses: $m_j = m$, where $j = 1, \dots, g$.
2. $R = \sqrt{g/\pi}$ and $\kappa_* = \pi m$.
3. $B(\mathbf{0}, R)$: closed disc of radius R centered at the origin $\mathbf{0}$.
4. The random point mass positions ξ_1, \dots, ξ_g are independent and uniformly distributed over $B(\mathbf{0}, R)$.

Now, normalize the random time delay function and random lensing map as follows:

$$T_{g,y}^*(\mathbf{x}) \equiv T_{g,y}(\mathbf{x}) + gm \log R, \quad \boldsymbol{\eta}_g^*(\mathbf{x}) \equiv \frac{\boldsymbol{\eta}_g(\mathbf{x})}{\sqrt{\log g}}.$$

Write the components of the random shear tensor due only to stars as follows:

$$\Gamma_{1,g}(\mathbf{x}) = \sum_{j=1}^g \frac{m[(U_j - u)^2 - (V_j - v)^2]}{[(U_j - u)^2 + (V_j - v)^2]^2}, \quad \Gamma_{2,g}(\mathbf{x}) = \sum_{j=1}^g \frac{2m(U_j - u)(V_j - v)}{[(U_j - u)^2 + (V_j - v)^2]^2}.$$

For fixed \mathbf{y} and \mathbf{x} , we denote the possible values of the previous random quantities as follows:

1. \mathfrak{t} = possible values of $T_{g,y}^*(\mathbf{x})$.
2. (\mathbf{h}, \mathbf{k}) = possible values of $\boldsymbol{\eta}_g^*(\mathbf{x})$.
3. (\mathbf{z}, \mathbf{w}) = possible values of $(\Gamma_{1,g}(\mathbf{x}), \Gamma_{2,g}(\mathbf{x}))$.
4. $\mathbf{G} = (\mathbf{z}^2 + \mathbf{w}^2)^{1/2}$ = possible values of the magnitude of the shear.

For the asymptotic p.d.f. of the normalized random lensing map, we shall need the quantities

$$\mathbf{a}_1 = \frac{(1 - \kappa_c + \gamma)u}{\sqrt{\log g}}, \quad \mathbf{a}_2 = \frac{(1 - \kappa_c - \gamma)v}{\sqrt{\log g}}, \quad \sigma_g^* = \frac{\kappa_*}{\sqrt{\pi}} \sqrt{\frac{\log(\mathbf{B} g^{1/2})}{\log g}}, \quad \mathbf{B} = \frac{2\sqrt{\pi}e^{1-\gamma_e}}{\kappa_*},$$

where γ_e is Euler's constant. For the asymptotic p.d.f. of the random shear, we shall use:

$$H_1(\mathbf{G}) = \kappa_*^2 \frac{9\mathbf{G}^2 - 6\kappa_*^2}{4(\kappa_*^2 + \mathbf{G}^2)^2} \quad (7)$$

and

$$H_2(\mathbf{G}; |\mathbf{x}|) = \frac{\kappa_* |\mathbf{x}|^2}{m} \frac{\kappa_*^2 (6\kappa_*^2 - 9\mathbf{G}^2)}{2(\kappa_*^2 + \mathbf{G}^2)^2} - \frac{\kappa_*^2 (8\kappa_*^4 - 24\kappa_*^2 \mathbf{G}^2 + 3\mathbf{G}^4)}{4(\kappa_*^2 + \mathbf{G}^2)^3} + \frac{15\kappa_*^4 (8\kappa_*^4 - 40\kappa_*^2 \mathbf{G}^2 + 15\mathbf{G}^4)}{32(\kappa_*^2 + \mathbf{G}^2)^4}. \quad (8)$$

Note that H_2 depends on $\kappa_* |\mathbf{x}|^2/m$, which is the mean number of point masses within the disc of radius $|\mathbf{x}|$ centered at the origin.

5.2 Asymptotic P.D.F.s of Random Time Delay Function, Random Lensing Map, and Random Shear

In 2009, AOP, Rider, and Teguiá [65,66] used a rigorous mathematical approach to characterize up to order three the asymptotic p.d.f.s of the microlensing normalized random time delay function, normalized random lensing map, and random shear:

Theorem 7 Fix $\mathbf{y} \in S$ and $\mathbf{x} = (u, v) \in B(\mathbf{0}, R)$. Then:

1. [65] **(Random Normalized Time Delay Function)** In the large g limit, the asymptotic p.d.f. of $T_{g,y}^*(x)$ takes the following form:

$$f_{T_{g,y}^*(\mathbf{x})}(\mathfrak{t}) = \left\{ \left(\frac{2}{m} \right)^g \frac{(\mathfrak{t} - d_1 - c)^{g-1}}{(g-1)!} \exp \left[-\frac{2(\mathfrak{t} - d_1 - c)}{m} \right], \quad \mathfrak{t} > d_1 + c \right\} + O(g^{-3/2}).$$

$$0, \quad \mathfrak{t} < d_1 + c$$

The first term of the p.d.f. is a Gamma distribution.

2. [65] **(Random Normalized Lensing Map)** In the large g limit, the asymptotic p.d.f. of $\boldsymbol{\eta}_g^*(\mathbf{x})$ takes the following form:

$$f_{\boldsymbol{\eta}_g^*(\mathbf{x})}(\mathbf{h}, \mathbf{k}) = \frac{e^{-\frac{(\mathbf{h} - \mathbf{a}_1)^2 + (\mathbf{k} - \mathbf{a}_2)^2}{2(\sigma_g^*)^2}}}{(\sqrt{2\pi}\sigma_g^*)^2} \left[1 - \kappa_* \frac{(\mathbf{h} - \mathbf{a}_1)u + (\mathbf{k} - \mathbf{a}_2)v}{\sigma_g^2} \right. \\ \left. + \frac{\kappa_*^2}{4\pi} \frac{((\mathbf{h} - \mathbf{a}_1)^2 + (\mathbf{k} - \mathbf{a}_2)^2 - 2(\sigma_g^*)^2)}{(\sigma_g^*)^4} \log(\log g) \right] + O\left(\frac{1}{\log^2 g}\right) \quad (9)$$

The first term of the p.d.f. is a bivariate Gaussian distribution, but the next two terms highlight that $\boldsymbol{\eta}_g^*(\mathbf{x})$ already becomes non-Gaussian for large finite g .

3. [66] **(Random Shear)** In the large g limit, the asymptotic p.d.f. of $(\Gamma_{1,g}^*(\mathbf{x}), \Gamma_{2,g}^*(\mathbf{x}))$ takes the following form:

$$f_{\Gamma_{1,g}(\mathbf{x}), \Gamma_{2,g}(\mathbf{x})}(\mathbf{z}, \mathbf{w}) = \frac{\kappa_*}{2\pi(\kappa_*^2 + \mathbf{G}^2)^{3/2}} \left[1 + \frac{H_1(\mathbf{G})}{g} + \frac{H_2(\mathbf{G}; |x|)}{g^2} \right] + O(g^{-3}), \quad (10)$$

where $\mathbf{G} = (\mathbf{z}^2 + \mathbf{w}^2)^{1/2}$ denotes the possible values of the magnitude of the shear. The first term of the p.d.f. is a stretched bivariate Cauchy distribution.

By equation (10), the asymptotic p.d.f. of the magnitude of the shear, namely, $\Gamma_g(\mathbf{x}) = \sqrt{\Gamma_{1,g}^2(\mathbf{x}) + \Gamma_{2,g}^2(\mathbf{x})}$, is given as follows [66]:

$$f_{\Gamma_g(\mathbf{x})}(\mathbf{G}) = \frac{\kappa_* \mathbf{G}}{(\kappa_*^2 + \mathbf{G}^2)^{3/2}} \left[1 + \frac{H_1(\mathbf{G})}{g} + \frac{H_2(\mathbf{G}; |x|)}{g^2} \right] + O(g^{-3}).$$

Remarks:

1. The first term in (9) was basically found in 1986 by Katz, Balbus, and Paczyński [38], who actually determined the first term of the p.d.f. of the bending angle due only to stars, namely, the p.d.f. of the random vector $\boldsymbol{\alpha}_g(\mathbf{x}) = \boldsymbol{\eta}_g(\mathbf{x}) - ((1 - \kappa_c + \gamma)\mathbf{u}, (1 - \kappa_c - \gamma)\mathbf{v})$.
2. The first term in (10) was found in 1984 by Nityananda and Ostriker [52].

Subsequent work in 2009 by Keeton [39] used semi-analytical and numerical methods to study the stochastic properties of the lens potential, deflection angle, and shear under different assumptions about the distributions of the stars' masses and positions.

5.3 Global Expected Number of Micro-Minima

Wambsganss, Witt, and Schneider 1992 [79] determined the limit $g \rightarrow \infty$ of the (global⁵) expected number \mathbf{E}_0 of minima in the *entire* plane \mathbb{R}^2 for microlensing without shear. This was extended to the case with shear in 2003 by Granot, Schechter, and Wambsganss [35]:

$$\mathbf{E}_0 = \frac{\kappa_*}{2\pi|(1 - \kappa_{\text{tot}})^2 - \gamma^2|} \int_{\mathcal{B}} \frac{(1 - \kappa_c)^2 - (\gamma + \mathbf{z})^2 - \mathbf{w}^2}{(\kappa_*^2 + \mathbf{G}^2)^{3/2}} d\mathbf{z}d\mathbf{w},$$

where $\kappa_{\text{tot}} = \kappa_* + \kappa_c$ and γ is same shear employed at the microlensing scale.

The value \mathbf{E}_0 resulting from the limit $g \rightarrow \infty$ is, of course, independent of g and can be treated as the first term in an asymptotic expansion in $1/g$. On the other hand, since the first term \mathbf{E}_0 is independent of g , if we have only the term \mathbf{E}_0 , then there is no way to know analytically the smallest g needed to lie within a certain approximation of the global expected number of micro-minima. This is especially important in numerical simulations. Therefore, we need to find more terms in the asymptotic expansion.

AOP, Rider and Teguiá 2009 [66] applied Theorem 6 and Theorem 7(3) to determine rigorously the global expected number of micro-minima up to three orders:

Theorem 8 [66] **(Global Expected Number of Micro-Minima)** *Let D be a closed disc and suppose that continuous matter is subcritical, i.e., $0 \leq \kappa_c < 1$. Then, in the large g limit, the first three asymptotic terms of the global expectation of the number of minimum images in D is given by.⁶*

$$\widehat{E}[N_{g,\min}(D, Y; \mathfrak{S})]_{\{\mathfrak{S}\}} = \frac{\kappa_* \mu_{D, \mathfrak{S}_0}}{2\pi} \int_{\mathcal{B}} \frac{(1 - \kappa_c)^2 - (\gamma + \mathbf{z})^2 - \mathbf{w}^2}{(\kappa_*^2 + \mathbf{G}^2)^{3/2}} \left[1 + \frac{H_1(\mathbf{G})}{g} + \frac{H_2(\mathbf{G}; a_0)}{g^2} \right] d\mathbf{z}d\mathbf{w} + O(g^{-3}), \quad (11)$$

where $\mu_{D, \mathfrak{S}_0} = \frac{|D|}{|\mathfrak{S}_0|}$, \mathcal{B} is a closed disc of radius $1 - \kappa_c$ centered at $(-\gamma, 0)$, and $a_0 = \frac{1}{|D|} \int_D |\mathbf{u}|^2 d\mathbf{u}$.

⁵ The terminology ‘‘global expected number of minima’’ was actually introduced in [66], where the difference between the expected number of minima and global expected number of minima was clarified.

⁶ The quantities H_1 and H_2 were defined in (7) and (8).

Theorem 8 gives us the leading three terms in an asymptotic expansion of the global expected number of micro-minima in any reference disc D , not necessarily in the entire plane. The first term in that expansion (11) is more general than E_0 because E_0 applies to the whole plane. A possible physical model for the factor μ_{D, \mathfrak{E}_0} in (11) is the macro-scale magnification given by:

$$\mu_{D, \mathfrak{E}_0} = \frac{1}{|(1 - \kappa_{\text{tot}})^2 - \gamma^2|}.$$

It is only in this case that the first term in (11) coincides with E_0 .

Another consequence of Theorem 8 is it enables us to estimate how small we can choose g in order to have the first three terms in the asymptotic expansion (11) lie within a certain percentage of the global expected number of micro-minima. Theorem 8 also shows us analytically how accurate an approximation the first term is to the exact global expectation by quantifying how the next two higher-order terms perturb the first one.

Remark: The third-order term in (11) depends on the mean number of point masses within the disc of radius $|\mathbf{x}|$ centered at the origin, namely, the quantity $\kappa_* |\mathbf{x}|^2/m$; compare equation (8).

6 Multiple Images in Optical Geometry

6.1 The Optical Metric and Fermat's Principle

The trajectories of spatial light rays can also be studied in optical geometry, which is conceptually between the thin-lens, weak-deflection approximation used in the previous sections and the full spacetime treatment of null geodesics. Optical geometry, which is also known as Fermat geometry or optical reference geometry, is a useful tool to investigate gravitational and inertial forces in General Relativity [4]. Recently, it has also been applied to field theory near black hole horizons by Gibbons and Warnick [30], and to analogue models of gravity in Finsler geometry by Gibbons, Herdeiro, Warnick and MCW [29].

Fermat's principle and optical geometry in the conformally stationary case was discussed in detail by Perlick [56]. To illustrate this approach, consider for simplicity a static spacetime metric

$$ds^2 = g_{00} (dt)^2 + g_{ij} dx^i dx^j,$$

where the summation convention is used, and a null curve parametrized by $0 \leq \nu \leq 1$, say, with tangent vector \mathbf{k} . Then the variational principle yields (e.g., Frankel [23]):

$$\delta t = \frac{1}{g(\frac{\partial}{\partial t}, \mathbf{k})} \int_0^1 g(\delta x, \nabla_{\mathbf{k}} \mathbf{k}) d\nu = 0,$$

if the null curve is in fact a null geodesic with $\nabla_{\mathbf{k}} \mathbf{k} = 0$. Hence, one obtains Fermat's principle of stationary arrival time, rather than stationary travel time as in the case of flat space used in the impulse approximation. Now recasting the spacetime line element as follows, we see that the spatial light rays are geodesics of the optical metric g^{opt} with Riemannian signature,

$$(dt)^2 = -\frac{g_{ij}}{g_{00}} dx^i dx^j \equiv g_{ij}^{\text{opt}} dx^i dx^j,$$

by Fermat's Principle.

6.2 Gauss-Bonnet and Lensed Images

Optical geometry offers a different perspective on image multiplicity in gravitational lensing, which is also partially topological. This can be understood with the Gauss-Bonnet Theorem, which connects the local optical geometry with global properties of the light rays. Gibbons [28] discussed this for cosmic strings, and this method was recently extended to spherically symmetric metrics by Gibbons and MCW [31] and Gibbons and Warnick [30]. In this approach, the occurrence of two images can be expressed as a digon of light rays:

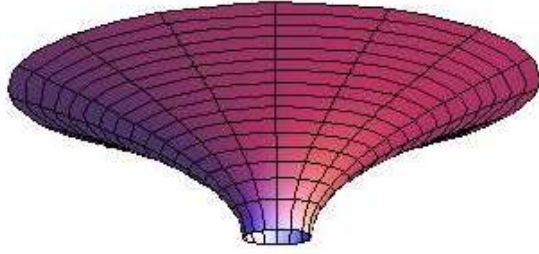


Fig. 3 Isometric embedding in \mathbb{R}^3 of the equatorial plane of the Schwarzschild solution in the optical metric. The waist occurs at the radius of the photon sphere, $r = 3m$. The Gaussian curvature is negative everywhere.

Theorem 9 [28, 31, 30] (**Light Ray Digons**) *Let $(S, g^{\text{opt}}$) be a totally geodesic, simply connected surface endowed with an optical metric g^{opt} and Gaussian curvature K . Let $D \subset S$ be a geodesic digon⁷ bounded by two light rays intersecting at the light source $s \in S$ and the observer $o \in S$ with corresponding positive interior angles θ_s and θ_o . Then:*

$$\theta_s + \theta_o = \int \int_D K dS.$$

Example: The Schwarzschild solution with mass parameter m is an instructive example. The equatorial plane in the optical metric outside the photon sphere is shown in Fig. 3, and it can be seen that the Gaussian curvature is negative everywhere. Indeed, a calculation of the Gaussian curvature gives

$$K = -\frac{2m}{r^3 \left(1 - \frac{2m}{r}\right)^{3/2}} \left(1 - \frac{3m}{2r}\right) < 0.$$

Spatial light rays, which are the geodesics of S , must therefore diverge locally, and the equation of the Theorem cannot be fulfilled. So the fact that two light rays can intersect at the source s and the observer o in Schwarzschild geometry shows that S cannot be simply connected, which indeed it is not because of the event horizon at $r = 2m$. Hence, the topological contribution to the Gauss-Bonnet theorem turns out to be essential for image multiplicity.

Example: Now consider the Plummer model with mass m_0 and scale radius r_0 . This is a reasonable model for an extended non-relativistic gravitational lens (i.e., a galaxy) which allows multiple imaging: three images are produced if the light source is in the maximal caustic domain. Of course, there is no event horizon in this model, so the surface S is simply connected, and the optical metric approaches that of the Schwarzschild solution with $K < 0$ at large radii r , since m_0 is finite. Therefore, the equation of the theorem holds, and we expect that the Gaussian curvature of the optical metric changes sign in order to allow for multiple images. A calculation of K to lowest order yields

$$K = -\frac{2m_0}{r_0^3} \left(1 + (r/r_0)^2\right)^{-\frac{3}{2}} \left(1 - \frac{3}{1 + (r/r_0)^2}\right) + O(m_0^2),$$

which confirms that $K > 0$ for small radii.

A more detailed analysis shows that the Gauss-Bonnet theorem can also be used to calculate deflection angles. In the case of the singular isothermal sphere, for instance, the optical metric describes a cone so that the gravitational deflection emerges as a consequence of the cone's deficit angle, rather like a spatial analogue of lensing by cosmic strings [31].

7 Multiple Images in Spacetime

7.1 Necessary and Sufficient Conditions for Multiple Images

The theories for spatial light rays provide useful frameworks for gravitational lensing, especially since the impulse approximation can easily be applied to models of astrophysical interest. However, the fundamen-

⁷ A *geodesic digon* in a lensing scenario is a polygon with two vertices, bounded by the two geodesics intersecting at the source and the observer.

tal arena of optics in General Relativity is of course spacetime. The study of wavefront singularities in spacetime was pioneered by Friedrich and Stewart [24], who classified stable singularities in Minkowski space and considered the relationship with the initial value problem in General Relativity. The general form of Fermat's Principle in spacetime was investigated by Kovner [43], and a precise proof for arbitrary Lorentzian manifolds (M, g) was first obtained by Perlick [55] in 1990. This also laid the foundation for a rigorous study of the conditions for multiple images in spacetime, which made an earlier result by Padmanabhan and Subramanian [54] more precise. Perlick showed that the existence of a conjugate point or a cut point along a null geodesic is a sufficient condition, which becomes necessary if further conditions on the topology or causal structure of M are imposed:

Theorem 10 [58] (**Multiple Images in Spacetime**) *Let (M, g) be a four-dimensional time-oriented Lorentzian manifold.*

1. **Sufficient Conditions:** *Let λ be a future-pointing null geodesic affinely parametrized by s , and fix $\lambda(s_1) = p \in M$.*
 - (a) *If there is a $s_2 > s_1$ such that $\lambda(s_2)$ is conjugate to $\lambda(s_1)$ along λ , then there is a timelike curve through each $\lambda(s), s > s_2$, which can be reached from p along another future-pointing null geodesic.*
 - (b) *If there is a $s_2 > s_1$ such that $\lambda(s_2)$ is the future cut point of p along λ , then there is a timelike curve through each $\lambda(s), s > s_2$, which can be reached from p along another future-pointing null geodesic.*
2. **Necessary Conditions:** *Fix a timelike curve γ and a point $p \in M$.*
 - (a) *If there are two future-pointing null geodesics from p to γ which are null homotopic, then there is a future-pointing null geodesic from p to γ which contains a point conjugate to p .*
 - (b) *If (M, g) is strongly causal and if there are two future-pointing null geodesics from p to γ , then the intersection with γ comes on or after the future cut point of p along at least one of the null geodesics.*

Having established conditions for existence, one can now proceed with counting results for null geodesics.

7.2 The Odd Number Theorem in a Spacetime Setting

The proofs of the Odd Number Theorem for single and multiple lens planes discussed in Sections 2 and 3 employ finite dimensional Morse theory in the impulse approximation. Interestingly, this result can also be extended to spacetime under certain assumptions. McKenzie 1985 showed this using the degree of a map between two spatial spheres, which requires stationarity of the spacetime, and gave a proof using Uhlenbeck's Morse theory for null geodesics on globally hyperbolic Lorentzian manifolds [48]. However, these conditions appear to be too restrictive for realistic spacetimes, as discussed by Gottlieb 1994 [34]. An extension to infinite dimensional Morse theory on the Hilbert space of null curves was developed Perlick 1995 [57] and Giannoni, Masiello and Piccione 1998 [27]. The resulting Morse relations have been applied by Giannoni and Lombardi [26] to prove a version of the Odd Number Theorem. In 2001, Perlick [59] defined the concept of a *simple lensing neighborhood*, which formalizes a physically meaningful lensing geometry to avoid some of the technical complexities, and proved the following spacetime version of the Odd Number Theorem:

Theorem 11 [59] (**Odd Number of Null Geodesics**) [59] *Let U be a simple lensing neighborhood in a four-dimensional time-oriented Lorentzian manifold (M, g) . Fix a point $p \in U$ and a timelike curve γ in U such that it has no endpoints on the boundary ∂U . If γ intersects neither p nor the caustic of the past light cone of p , then the number of past-pointing null geodesics from p to γ completely within U is finite and odd.*

A rigorous treatment of the optics in a spacetime setting can be found in Perlick [60].

8 Global Magnification Relations for Special Lens Models

In gravitational lensing, when a source gives rise to multiple images, the magnifications of these images often obey certain relations. The simplest example of such a relation is provided by a single point-mass

lens. In this setting a source gives rise to two lensed images, and it can be shown that their signed magnifications always sum to unity:

$$\mu_1 + \mu_2 = 1 \quad (\text{one point mass})$$

(e.g., [64], p. 191). The surprising fact about this result is that it holds irrespectively of the mass of the point mass and its position on the lens plane. It is also a “global” relation, by which is meant that it involves all of the images of a given source and not merely a subset of them. Witt and Mao 1995 [83] generalized this result to a two point-mass lens. They showed that for a source lying anywhere inside the caustic curve, a region which gives rise to five lensed images (the maximum number in this case), the sum of the signed magnifications of these images is also unity:

$$\mu_1 + \mu_2 + \mu_3 + \mu_4 + \mu_5 = 1 \quad (\text{two point masses}).$$

Like its predecessor, this relation is “global” and holds irrespectively of the lens’s configuration, provided the source lies inside the region giving rise to the maximum number of images. Rhie 1997 [69] subsequently extended this result to N point masses. Dalal 1998 [19] and Witt and Mao 2000 [84] then showed that other common lens models, such as singular isothermal spheres and ellipses (SISs and SIEs) and elliptical power-law potentials, possess similar global magnification relations, even when these models include shear.

Dalal and Rabin 2001 [20] provided a residue approach that systematized and expanded on the above work. They began with the Euler trace formula, which they proved using residue calculus. The Euler trace formula identifies sums of magnifications as coefficients of certain coset polynomials; we shall return to this in Section 10.3 below. The method in [20] uses meromorphic differential forms in several complex variables. By considering a meromorphic 2-form on \mathbb{C}^2 consisting of polynomials whose common zeros are the image positions of the lensing map, the authors were able to use the Global Residue Theorem, which states that on compact manifolds the sum of all the residues of a meromorphic form vanishes. This allows one to replace the common zeros of a form in \mathbb{C}^2 , viewed as a subset of the compact manifold \mathbb{CP}^2 , by minus the sum of residues at infinity in \mathbb{CP}^2 . In this way magnification sums were transformed to a condition about the behavior of the lens equation at infinity. Their results are summarized in the following theorem:

Theorem 12 [20] *The models listed below possess the following zeroth and first magnification moment relations:*

| Model | $\sum_j \mu_j$ | $\sum_j \mu_j z_j$ |
|-----------------------------------|--------------------------|--|
| <i>point masses</i> | 1 | $z_s + \sum_j \frac{m_j}{\bar{z}_s - \bar{z}_j}$ |
| <i>point masses + shear</i> | $\frac{1}{1 - \gamma^2}$ | $\frac{z_s + \gamma \bar{z}_s}{(1 - \gamma^2)^2}$ |
| <i>SIE</i> | 2 | $2z_s$ |
| <i>SIE + elliptical potential</i> | 1 | $z_s + 2\gamma \bar{z}_s - \frac{\bar{z}_s^3}{32 b^2 \gamma^2}$ |
| <i>SIS + shear</i> | $\frac{2}{1 - \gamma^2}$ | $\frac{2(z_s + \gamma \bar{z}_s)}{(1 - \gamma^2)^2}$ |
| <i>SIE + shear</i> | $\frac{2}{1 - \gamma^2}$ | $\frac{2(z_s + \gamma e^{2i\theta} \gamma \bar{z}_s)}{(1 - \gamma^2)^2}$ |

Notation: m_j is the mass of j th point mass, γ is the shear with orientation θ_γ , and z_j and z_s are, respectively, the position of the j th lensed image and the position of the source using complex variables.

Residue calculus methods were also used by Hunter and Evans 2001 [37], wherein magnifications of images were realized as residues of complex integrands. By Cauchy’s theorem, sums of magnifications are then equivalent to a contour integral. This method was used to derive magnification relations for elliptical power-law potentials which expanded upon the work of [84]. As first shown in [84], for an elliptical power law potential $\psi(\mathbf{x}) \propto (u^2 + v^2 q^{-2})^{b/2}$, where q is the ratio of the minor to major axes, the total signed magnification denoted by \mathbf{B} is exactly $\mathbf{B} = 2/(2 - b)$ for the cases $b = 0, 1$; for other values, it is an approximation. The contour integral method used in [37, 21] covered not only all cases when \mathbf{B} is an integer, including second and third magnification moments, reciprocal moments, and random shear, but also cases with non-integer values of \mathbf{B} as well. In 2002, Evans and Hunter [21] extended their results in [37] to include elliptical power-law potentials with a core radius, and calculated magnification invariants for subsets of the images with even and odd parities.

9 Local Magnification Relations: Caustics up to Codimension 3

9.1 Quantitative Fold and Cusp Magnification Relations: Single Plane Lensing

All of the above magnification relations are “global” because they involve all the lensed images of a given source. But they are not *universal* because their relations were derived in the context of specific types of lens models (point-mass lenses, SIEs, etc.) There is another type of magnification relation, a so-called “local” magnification relation, that *is* universal in the sense that it holds for a generic family of lens models. It is called a “local” relation because it holds for a subset of the total number of lensed images. Such relations arise when the source lies close to a caustic singularity. The two simplest types of such singularities are the fold and the cusp. For a source near a fold, there will be two images straddling the critical curve, while for a source near a cusp, there will be a triplet of images. Interestingly, the signed magnifications of this doublet and triplet always sum to zero (e.g., Blandford and Narayan 1986 [15], Schneider and Weiss 1992 [74], and Zakharov 1999 [85]):

$$\mu_1 + \mu_2 = 0 \text{ (fold)}, \quad \mu_1 + \mu_2 + \mu_3 = 0 \text{ (cusp)}. \quad (12)$$

These relations are important in gravitational lensing because they can be used to detect dark substructure in galaxies with “anomalous” flux ratios. These anomalies arise as follows. For quasars with four lensed images, it is often the case that the *smooth* mass densities used to model the galaxy lens reproduce the number and positions of the lensed images, but fail to reproduce the image flux ratios. Mao and Schneider 1998 [47] showed that in such situations the cusp magnification relation (12) fails. They attributed this failure to the assumption of smoothness in the galaxy lens, and argued that this smoothness breaks down on the scale of the image separation. This suggests the presence of substructure in the galaxy lens. The possibility of this became even more intriguing when Metcalf and Madau 2001 [49] and Chiba 2002 [18] showed that dark matter would be a natural candidate for this substructure.

Being able to identify which anomalous lenses have substructure now became a priority. Keeton, Gaudi and AOP in 2003 [40] and 2005 [41] developed a rigorous framework by which to do so, using the observable quantities:

$$R_{\text{fold}} \equiv \frac{\mu_1 + \mu_2}{|\mu_1| + |\mu_2|} = \frac{F_1 - F_2}{F_1 + F_2}, \quad R_{\text{cusp}} \equiv \frac{\mu_1 + \mu_2 + \mu_3}{|\mu_1| + |\mu_2| + |\mu_3|} = \frac{F_1 - F_2 + F_3}{F_1 + F_2 + F_3},$$

where F_i is the observable flux of image i . The importance of these quantities is as follows. If a source lies sufficiently close to a fold or cusp caustic, then (12) predicts that R_{fold} and R_{cusp} should vanish. If R_{fold} and R_{cusp} deviate significantly from zero (Monte Carlo methods were used to determine what constituted a significant deviation), then that would indicate the presence of substructure in that particular lens. On this basis it was shown in [40, 41] that for the multiply imaged lens systems they analyzed, 5 of the 12 fold-image lenses and 3 of the 4 cusp-image lenses showed evidence of substructure.

9.2 Quantitative Elliptic and Hyperbolic Umbilics' Magnification Relations: Single Plane Lensing

Consider a family of time delay functions $T_{c,\mathbf{y}}$ which induces a corresponding family of lensing maps η_c . Here \mathbf{y} is the source position on the source plane and the parameter c can be any physical input, such as the core radius or external shear.⁸ Using rigid coordinate transformations and Taylor expansions, the *universal, quantitative* form of the lensing map can be derived in a neighborhood of a caustic (see [72,64]). As mentioned above, the quantitative forms of lensing maps near fold and cusp caustics obey the fold and cusp magnification relations (12). Aazami and AOP 2009 [1] showed recently that the quantitative forms of lensing maps near certain *higher-order* caustic singularities, namely the elliptic and hyperbolic umbilics, also satisfy magnification relations analogous to (12). Their work is summarized by the following theorem:

Theorem 13 [1] *For any of the smooth generic family of time delay functions $T_{c,\mathbf{y}}$ corresponding to the elliptic umbilic or hyperbolic umbilic caustic singularities, and for any source position in the indicated region, the following results hold:*

1. D_4^- (Elliptic Umbilic) *satisfies the following magnification relation in its four-image region:*

$$\mu_1 + \mu_2 + \mu_3 + \mu_4 = 0.$$

2. D_4^+ (Hyperbolic Umbilic) *satisfies the following magnification relation in its four-image region:*

$$\mu_1 + \mu_2 + \mu_3 + \mu_4 = 0.$$

An application of this theorem to substructure studies was also given in [1], using the hyperbolic umbilic (D_4^+) in particular. Analogous to the observables R_{fold} and R_{cusp} , the authors considered the following quantity:

$$R_{\text{h.u.}} \equiv \frac{\mu_1 + \mu_2 + \mu_3 + \mu_4}{|\mu_1| + |\mu_2| + |\mu_3| + |\mu_4|} = \frac{F_1 - F_2 + F_3 - F_4}{F_1 + F_2 + F_3 + F_4}.$$

By Theorem 13, $R_{\text{h.u.}}$ should vanish for a source lying sufficiently close to a hyperbolic umbilic caustic singularity and lying in the four-image region. One advantage of $R_{\text{h.u.}}$ is that it incorporates a larger number of images than R_{fold} and R_{cusp} , and also applies to image configurations that cannot be classified as fold doublets or cusp triplets. In fact recent work has shown that higher-order caustics like the hyperbolic umbilic can be exhibited by lens galaxies. Evans and Witt 2001 [22], Shin and Evans 2007 [75], and Orban de Xivry and Marshall 2009 [53] have shown that realistic lens models can exhibit swallowtail (A_5) and butterfly caustics (A_4), as well as elliptic umbilics (D_4^-) and hyperbolic umbilics (D_4^+). It is hoped that such lensing effects will be seen by the Large Synoptic Survey Telescope, and thus that higher-order relations such as $R_{\text{h.u.}}$ will become applicable in the near future.

An example of the multiple imaging, critical curves, and caustic curves due to a hyperbolic umbilic (D_4^+) is shown in Figure 4.

9.3 Universal Local Magnification Relations: Generic Caustics up to Codimension 3

9.3.1 Preliminaries: Lensed Images and Magnification for Generic Mappings

Consider a smooth, n -parameter family $F_{\mathbf{c},\mathbf{s}}(\mathbf{x})$ of functions on an open subset of \mathbb{R}^2 that induces a smooth $(n-2)$ -parameter family of mappings $\mathbf{f}_{\mathbf{c}}(\mathbf{x})$ between planes ($n \geq 2$). The functions $F_{\mathbf{c},\mathbf{s}}$ are used to construct a *Lagrangian submanifold* that is projected into the n -dimensional space $\{\mathbf{c}, \mathbf{s}\} = \mathbb{R}^{n-2} \times \mathbb{R}^2$; the projection itself is called a *Lagrangian map*. The critical values of this projection will then comprise the caustics of $\mathbf{f}_{\mathbf{c}}$ (e.g., Golubitsky and Guillemin 1973 [33], Majthay 1985 [45], Castrigiano and Hayes 1993 [17], and [64, pp. 276-86]). Arnold classified all stable simple Lagrangian map-germs of n -dimensional Lagrangian submanifolds by their generating family $F_{\mathbf{c},\mathbf{s}}$ ([6], Arnold, Gusein-Zade, and Varchenko I 1985 [8, p. 330-31], and [64, p. 282]).

Given $\mathbf{f}_{\mathbf{c}}(\mathbf{x}) = \mathbf{s}$, we call $\mathbf{x} \in \mathbb{R}^2$ a *lensed image* of the *source (or target) point* $\mathbf{s} \in \mathbb{R}^2$; note that our lensed images are never complex-valued. Equivalently, lensed images are critical points of $F_{\mathbf{c},\mathbf{s}}$, relative

⁸ There is at most one universal unfolding parameter c for caustics up to codimension 3.

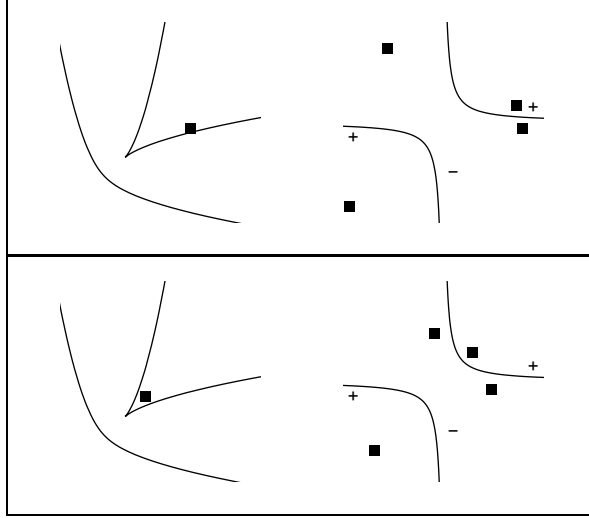


Fig. 4 Multiple images of a source inside a cross section of a hyperbolic umbilic caustic in lensing. In each panel, the figure on the left depicts the caustic curve with source position (solid box) in the light source plane, while the figure on the right shows the critical curve with corresponding image positions (solid boxes) in the lens plane. The + sign indicates that only minimum and maximum images lie in the given region and the – sign labels a region where only saddle images occur. Credits: Figure from [1].

to a gradient in \mathbf{x} . Next, we define the *signed magnification* $\mathfrak{M}(\mathbf{x}_i; \mathbf{s})$ at a critical point \mathbf{x}_i of $F_{\mathbf{c}, \mathbf{s}}$ to be the reciprocal of the Gaussian curvature at the point $(\mathbf{x}_i, F_{\mathbf{c}, \mathbf{s}}(\mathbf{x}_i))$ in the graph of $F_{\mathbf{c}, \mathbf{s}}$:

$$\mathfrak{M}(\mathbf{x}_i; \mathbf{s}) = \frac{1}{\text{Gauss}(\mathbf{x}_i, F_{\mathbf{c}, \mathbf{s}}(\mathbf{x}_i))}.$$

The advantage of this definition is it makes clear that the signed magnification invariants are *geometric* invariants. The signed magnification is expressible in terms of $\mathbf{f}_{\mathbf{c}}$ since $\text{Gauss}(\mathbf{x}_i, F_{\mathbf{c}, \mathbf{s}}(\mathbf{x}_i)) = \det[\text{Hess } F_{\mathbf{c}, \mathbf{s}}](\mathbf{x}_i)$ and each $\mathbf{f}_{\mathbf{c}}$ satisfies $\det[\text{Jac } \mathbf{f}_{\mathbf{c}}] = \det[\text{Hess } F_{\mathbf{c}, \mathbf{s}}]$. It follows that

$$\mathfrak{M}(\mathbf{x}_i; \mathbf{s}) = \frac{1}{\det[\text{Jac } \mathbf{f}_{\mathbf{c}}](\mathbf{x}_i)},$$

which is the more common definition of magnification. If $\det[\text{Jac } \mathbf{f}_{\mathbf{c}}](\mathbf{x}) = 0$, then \mathbf{x} is called a *critical point* of $\mathbf{f}_{\mathbf{c}}$. The collection of such points form curves called *critical curves*. The target $\mathbf{f}_{\mathbf{c}}(\mathbf{x})$ of a critical point \mathbf{x} is called a *caustic point*. Though these typically form curves as well, they could also be isolated points. Since there are caustic curves for each value of the parameters \mathbf{c} , varying these parameters traces out a caustic surface, called a *big caustic*, in the larger space $\{\mathbf{s}, \mathbf{c}\} = \mathbb{R}^n$. An example of critical and caustic curves is shown in Figure 4 for the hyperbolic umbilic (D_4^+), along with various source and image configurations.

9.3.2 Universal Magnification Relations for Generic Caustics Up to Codimension 3

The following theorem about magnification relations for generic caustics up to codimension 3 was established by Aazami and AOP in 2009 [1]:

Theorem 14 [1] *For any of the smooth generic families of functions $F_{\mathbf{c}, \mathbf{s}}$ (or the induced general mappings $\mathbf{f}_{\mathbf{c}}$) giving rise to a caustic of codimension up to 3, and for \mathbf{s} , any non-caustic point in the n -image region, the following holds for the image magnifications $\mathfrak{M}_i \equiv \mathfrak{M}(\mathbf{x}_i; \mathbf{s})$:*

$$\sum_{i=1}^n \mathfrak{M}_i = 0,$$

where $n = 2$ for a fold, $n = 3$ for a cusp, $n = 4$ for a swallowtail, elliptic umbilic, or hyperbolic umbilic.

The proofs of Theorems 13 and 14 in [1], including the subsequent shorter proof in [2], are algebraic in nature and the method will be highlighted in Section 10.3.

After [1] appeared, an alternative proof was given by MCW 2009 [81] that introduced new Lefschetz fixed point technology in gravitational lensing, clarifying an earlier approach [80]. The next section overviews the method in [81].

9.4 A Lefschetz Fixed Point Approach to Theorem 13 and Theorem 14

We first review some needed basics from Lefschetz fixed point theory and then outline how it can be used to prove the aforementioned theorems.

9.4.1 Holomorphic Lefschetz fixed point theory.

If $f : M \rightarrow M$ is a smooth map on a compact manifold M , then its fixed points are $\text{fix}(f) = \{x \in M : f(x) = x\}$, that is, the intersection of the graph $\{(x, f(x))\} \in M \times M$ with the diagonal $\{(x, x)\} \in M \times M$. Fixed point theory, then, connects local properties of the fixed points, called fixed point indices, with global properties of f and M . In the case of a real manifold M , this is called the *Lefschetz number* $L(f)$, which is a homotopy invariant because f induces a map on the space of closed forms and hence on the cohomology classes of M . For complex M and holomorphic f , the relationship between the analogous holomorphic Lefschetz number $L_{\text{hol}}(f)$ and the local fixed point indices is called *holomorphic Lefschetz fixed point formula*. The Lefschetz fixed point formulas are well-defined provided that the intersections are transversal, and can be regarded as special cases of the Atiyah-Bott Theorem [10,11].

To illustrate this concept, we now discuss polynomial maps on the Riemann sphere $\hat{\mathbb{C}} = \mathbb{CP}^1 = \mathbb{C} \cup \{\infty\}$ as an instructive example. Here, the holomorphic Lefschetz fixed point formula is also known as the Rational Fixed Point Theorem, which has important applications in complex dynamics (see, for example, the discussion by Milnor [50]):

Theorem 15 (Rational Fixed Point Theorem) *Let $f : \hat{\mathbb{C}} \rightarrow \hat{\mathbb{C}}$ be a rational map which is not the identity. Then:*

$$1 = \sum_{z \in \text{fix}(f)} \frac{1}{1 - \frac{df}{dz}}.$$

Here, the holomorphic Lefschetz number for complex projective space is $L_{\text{hol}}(f) = 1$. To see why this is true, recall that a rational map on the Riemann sphere can always be extended to a holomorphic map; then we can choose local holomorphic coordinates so that $z = 0$ for some fixed point and write $f(z) = \frac{df}{dz}(0)z + O(z^2)$ by holomorphicity. Hence,

$$\frac{1}{(1 - \frac{df}{dz})(0)} = \frac{1}{2\pi i} \oint_{\mathbb{C}} \frac{dz}{z - f(z)},$$

where \mathbb{C} is a loop enclosing only the fixed point at the origin. We may take f to be bounded so that

$$\frac{1}{z - f(z)} - \frac{1}{z} = \frac{f(z)}{z(z - f(z))} \approx \frac{f(\infty)}{z^2} \rightarrow 0 \text{ as } z \rightarrow \infty. \quad (13)$$

Using these results, if we now extend the loop \mathbb{C} to \mathbb{C}_{∞} of infinite radius enclosing all fixed points of f , then

$$\sum_{z \in \text{fix}(f)} \frac{1}{1 - \frac{df}{dz}} = \frac{1}{2\pi i} \oint_{\mathbb{C}_{\infty}} \frac{dz}{z - f(z)} = \frac{1}{2\pi i} \oint_{\mathbb{C}_{\infty}} \frac{dz}{z} = 1$$

as required, since the integral of (13) vanishes [50].

For a general complex manifold M with dimension d , the holomorphic Lefschetz formula is (see Griffiths and Harris [36], for instance)

$$L_{\text{hol}}(f) = \sum_{z \in \text{fix}(f)} \frac{1}{\det[I_d - D_f]}, \quad (14)$$

where I_d is the d -dimensional identity matrix and D_f is the matrix of first derivatives with respect to local holomorphic coordinates. Again, the transversality condition can be expressed as the requirement that the fixed point indices be well-defined, that is, $\det[I_d - D_f] \neq 0$.

| Singularity | $f_1^{\mathbb{C}}, f_2^{\mathbb{C}}$ | $\deg(f_1^{\mathbb{C}}), \deg(f_2^{\mathbb{C}})$ | n |
|----------------------------------|---|--|-----|
| Fold | z_1, z_2^2 | 1, 2 | 2 |
| Cusp | $z_1, z_1 z_2 + z_2^3$ | 1, 3 | 3 |
| Swallowtail | $z_1 z_2 + c z_1^2 + z_1^4, z_2$ | 4, 1 | 4 |
| Elliptic umbilic | $3z_2^2 - 3z_1^2 - 2c z_1, 6z_1 z_2 - 2c z_2$ | 2, 2 | 4 |
| Hyperbolic umbilic | $-3z_1^2 - c z_2, -3z_2^2 - c z_1$ | 2, 2 | 4 |
| Elliptic umbilic (lensing map) | $z_1^2 - z_2^2, -2z_1 z_2 + 4c z_2$ | 2, 2 | 4 |
| Hyperbolic umbilic (lensing map) | $z_1^2 + 2c z_2, z_2^2 + 2c z_1$ | 2, 2 | 4 |

Table 1 Components of the complex maps $\mathbf{f}_c^{\mathbb{C}}(z_1, z_2)$ for generic singularities up to codimension three, their degrees and the numbers n of real solutions in the maximal caustic domains at finite positions. Here c denotes a control parameter. The lower section lists the corresponding properties for the quantitative elliptic and hyperbolic umbilics for a lensing map.

9.4.2 Application to Theorems 13 and 14

We now outline the Lefschetz fixed point proof of Theorem 14. In the present approach (compare Atiyah and Bott [11]), all real solutions $\mathbf{f}_c(x_1, x_2) = (s_1, s_2)$ are treated as the real fixed points of a suitable complex map. So, first, we need to find a complexification that allows the application of the holomorphic Lefschetz fixed point formula. The standard complexification $(x_1, x_2) \mapsto x_1 + ix_2$ does not yield holomorphic maps, but this problem can be circumvented, at the expense of the dimension, by treating $(x_1, x_2) \equiv (z_1, z_2)$ as independent complex variables on \mathbb{C}^2 . The corresponding complex generic maps $\mathbf{f}_c^{\mathbb{C}} = (f_1^{\mathbb{C}}, f_2^{\mathbb{C}}) : \mathbb{C}^2 \rightarrow \mathbb{C}^2$ are shown in Table 1, and the maximum number of solutions of $f_1^{\mathbb{C}}(z_1, z_2) = s_1, f_2^{\mathbb{C}}(z_1, z_2) = s_2$, possibly complex, is $\deg(f_1^{\mathbb{C}}) \deg(f_2^{\mathbb{C}})$ by Bézout's Theorem. Now, since Table 1 shows that this is always equal to the maximum number n of real and finite solutions, we see that our complex formalism gives the usual real solutions in the maximal caustic domain, as required. Next, one can define the map $f = (f_1, f_2) = (z_1 - f_1^{\mathbb{C}} + y_1, z_2 - f_2^{\mathbb{C}} + y_2)$ on \mathbb{C}^2 such that its fixed points are in fact those solutions. Hence, by construction, f is holomorphic and has no fixed points at infinity. Notice also that, at these fixed points,

$$\frac{1}{\det[I_2 - D_f]} = \frac{1}{\det[\text{Jac } \mathbf{f}_c]} = \mathfrak{M}. \quad (15)$$

Although this looks rather suggestive, we cannot apply the holomorphic Lefschetz fixed point formula directly to f , since \mathbb{C}^2 is not compact. However, one can rewrite f in homogeneous coordinates (Z_0, Z_1, Z_2) , where $z_1 = Z_1/Z_0$ and $z_2 = Z_2/Z_0$ for $Z_0 \neq 0$, and consider the a map $F = (F_0 : F_1 : F_2)$ on $\mathbb{C}\mathbb{P}^2$, which is of course compact, where

$$\begin{aligned} F_0 &= Z_0^m, \\ F_1 &= Z_1 Z_0^{m-1} - Z_0^{m-\deg(f_1^{\mathbb{C}})} f_1^{\mathbb{C}}(Z_0, Z_1, Z_2) + y_1 Z_0^m, \\ F_2 &= Z_2 Z_0^{m-1} - Z_0^{m-\deg(f_2^{\mathbb{C}})} f_2^{\mathbb{C}}(Z_0, Z_1, Z_2) + y_2 Z_0^m, \end{aligned}$$

and $m = \max(\deg(f_1^{\mathbb{C}}), \deg(f_2^{\mathbb{C}})) \geq 2$. Thinking of $\mathbb{C}\mathbb{P}^2 = \mathbb{C}^2 \cup \mathbb{C}\mathbb{P}^1$, with $\mathbb{C}^2 : Z_0 = 1, \mathbb{C}\mathbb{P}^1 : Z_0 = 0$, we recover $F|_{\mathbb{C}^2} = f$. Also, F is holomorphic since f has no fixed points at infinity. Finally, the holomorphic Lefschetz fixed point formula (14) applies to F and to $F|_{\mathbb{C}\mathbb{P}^1}$, where $L_{\text{hol}} = 1$ as shown in Section 9.4.1. Hence, using (15), we obtain $1 = \sum_{i=1}^n \mathfrak{M}_i + 1$. This shows that the universal magnification invariant is zero for the generic cases in Theorem 14, which can now be interpreted as a difference of two Lefschetz numbers.

For the quantitative case a similar argument yields a proof of Theorem 13; the lower section of Table 1 shows that the properties of the quantitative elliptic and hyperbolic umbilics for lensing maps allow a construction as discussed in Section 9.4.2, in exactly the same way as for the corresponding generic maps.

Remark: The above fixed point approach to lensing should not be confused with the one studied by AOP and Wicklin 1998 [67], where fixed points of the lensing map were explored to determine source positions that have a lensed image coinciding with the unlensed angular position of the source. It is also interesting to note that the technical transversality condition mentioned in Section 9.4.1 simply becomes $|\mu| < \infty$ in the lensing context, that is, the usual condition for regular images.

| Class | $F_{\mathbf{c},\mathbf{s}}(x_1, x_2)$ $\mathbf{f}_{\mathbf{c}}(x_1, x_2)$ |
|-------------------------|---|
| A_n ($n \geq 2$) | $\pm x_1^{n+1} \pm x_2^2 + c_{n-1}x_1^{n-1} + \cdots + c_3x_1^3 + s_2x_1^2 - s_1x_1 \pm s_2x_2$ $(\pm(n+1)x_1^n + (n-1)c_{n-1}x_1^{n-2} + \cdots + 3c_3x_1^2 \mp 4x_2x_1, \mp 2x_2)$ |
| D_n ($n \geq 4$) | $x_1^2x_2 \pm x_2^{n-1} + c_{n-2}x_2^{n-2} + \cdots + c_2x_2^2 - s_2x_2 - s_1x_1$ $(2x_1x_2, x_1^2 \pm (n-1)x_2^{n-2} + (n-2)c_{n-2}x_2^{n-3} + \cdots + 2c_2x_2)$ |
| E_6 | $x_1^3 \pm x_2^4 + c_3x_1x_2^2 + c_2x_2^2 + c_1x_1x_2 - s_2x_2 - s_1x_1$ $(3x_1^2 + c_3x_2^2 + c_1x_2, \pm 4x_2^3 + 2c_3x_1x_2 + 2c_2x_2 + c_1x_1)$ |
| E_7 | $x_1^3 + x_1x_2^3 + c_4x_2^4 + c_3x_2^3 + c_2x_2^2 + c_1x_1x_2 - s_2x_2 - s_1x_1$ $(3x_1^2 + x_2^3 + c_1x_2, 3x_1x_2^2 + 4c_4x_2^3 + 3c_3x_2^2 + 2c_2x_2 + c_1x_1)$ |
| E_8 | $x_1^3 + x_2^5 + c_5x_1x_2^3 + c_4x_1x_2^2 + c_3x_2^3 + c_2x_2^2 + c_1x_1x_2 - s_2x_2 - s_1x_1$ $(3x_1^2 + c_5x_2^3 + c_4x_2^2 + c_1x_2, 5x_2^4 + 3c_5x_1x_2^2 + 2c_4x_1x_2 + 3c_3x_2^2 + 2c_2x_2 + c_1x_1)$ |

Table 2 The left column indicates the A, D, E type of the Coxeter-Dynkin diagram or generic caustic. The right column lists the associated universal local forms of the smooth $(n-1)$ -parameter family of general functions $F_{\mathbf{c},\mathbf{s}}$, along with their $(n-3)$ -parameter family of induced general maps $\mathbf{f}_{\mathbf{c}}$ between planes—see the two-component expressions (\dots, \dots) . The given classification is due to Arnold 1973 [6]. Credits: Table from [3].

10 Universal Local Magnification Relations: Generic Caustics Beyond Codimension 3

10.1 The Infinite Family of A, D, E Caustics

In Arnold's classification of stable simple Lagrangian map-germs of n -dimensional Lagrangian submanifolds by their generating family $F_{\mathbf{c},\mathbf{s}}$ [6] (also, see Arnold, Gusein-Zade, and Varchenko [8, p. 330-31]), he found a deep connection between his classification and the Coxeter-Dynkin diagrams of the simple Lie algebras of types A_n ($n \geq 2$), D_n ($n \geq 4$), E_6, E_7, E_8 . This classification is shown in Table 2 [3] and is known as the A, D, E classification of caustic singularities.

The generic caustic singularities up to codimension 5 are given as follows in the Arnold A, D, E notation, where the numbers nD in parentheses indicate the codimension:

1. (1D) A_2 is a fold.
2. (2D) A_3 is a cusp.
3. (3D) A_4 is a swallowtail, D_4^- an elliptic umbilic, and D_4^+ a hyperbolic umbilic.
4. (4D) A_5 is a butterfly, D_5 a parabolic umbilic.
5. (5D) A_6 is a wigwam, D_6^- a 2nd elliptic umbilic, D_6^+ a 2nd hyperbolic umbilic, E_6 symbolic umbilic.

Remark: Up to codimension 5, all Lagrangian maps can be approximated by stable Lagrangian map-germs [6]. However, for codimension 6 or higher, this is no longer the case; unstable mappings form an open dense set [6,8].

10.2 Universal Magnification Relations for the Family of A, D, E Caustics

In 2009, Aazami and AOP [3] proved a universal local magnification relation theorem for generic general mappings between planes exhibiting *any* caustic singularity appearing in Arnold's A, D, E family:

Theorem 16 [3] *For any of the generic smooth $(n-1)$ -parameter family of general functions $F_{\mathbf{c},\mathbf{s}}$ (or induced general mappings $\mathbf{f}_{\mathbf{c}}$) in the A, D, E classification, and for any non-caustic point \mathbf{s} in the indicated region, the following results hold for the magnification $\mathfrak{M}_i \equiv \mathfrak{M}(\mathbf{x}_i; \mathbf{s})$:*

1. A_n ($n \geq 2$) obeys the magnification relation in the n -image region: $\sum_{i=1}^n \mathfrak{M}_i = 0$,
2. D_n ($n \geq 4$) obeys the magnification relation in the n -image region: $\sum_{i=1}^n \mathfrak{M}_i = 0$,
3. E_6 obeys the magnification relation in the six-image region: $\sum_{i=1}^6 \mathfrak{M}_i = 0$,
4. E_7 obeys the magnification relation in the seven-image region: $\sum_{i=1}^7 \mathfrak{M}_i = 0$,
5. E_8 obeys the magnification relation in the eight-image region: $\sum_{i=1}^8 \mathfrak{M}_i = 0$.

Remark: Theorem 16 does not follow directly from the Euler-Jacobi formula, the multi-dimensional residue integral approach [20], or the Lefschetz fixed point theory method [81], because some of the singularities have fixed points at infinity.

10.3 On the Proof of Theorem 16

The proof of Theorem 16 given in [3] employed the Euler trace formula. This formula was shown by Aazami and AOP [2] in 2009 to be a corollary of a more general result they established about polynomials:

Theorem 17 [2] *Let $\varphi(x) = a_n x^n + \dots + a_1 x + a_0 \in \mathbb{C}[x]$ be any polynomial with distinct roots x_i , and let $h(x) \in R$ be any rational function, where R is the subring of rational functions that are defined at the roots of $\varphi(x)$. Let*

$$h_*(x) = c_{n-1}x^{n-1} + \dots + c_1x + c_0$$

be the unique polynomial representative of the coset $\overline{h(x)} \in R/(\varphi(x))$ and let

$$r(x) = b_{n-1}x^{n-1} + \dots + b_1x + b_0$$

be the unique polynomial representative of the coset $\overline{\varphi'(x)h(x)} \in R/(\varphi(x))$. Then the coefficients of $r(x)$ are given in terms of the coefficients of $h_(x)$ and $\varphi(x)$ by the following recursive relation:*

$$b_{n-i} = c_{n-1}b_{n-i,n-1} + \dots + c_1b_{n-i,1} + c_0b_{n-i,0} \quad i = 1, \dots, n,$$

with

$$\begin{cases} b_{n-i,0} = (n - (i - 1)) a_{n-(i-1)}, & i = 1, \dots, n, \\ b_{n-i,k} = -\frac{a_{n-i}}{a_n} b_{n-1,k-1} + b_{n-(i+1),k-1}, & i = 1, \dots, n, \quad k = 1, \dots, n - 1, \end{cases}$$

where $b_{-1,k-1} \equiv 0$.

Corollary 3 (Euler Trace Formula) *Assume the hypotheses and notation of Theorem 17. For any rational function $h(x) \in R$, the following holds:*

$$\sum_{i=1}^n h(x_i) = \frac{b_{n-1}}{a_n}.$$

See [20] for a residue calculus approach to the Euler trace formula.

One can now show that the total signed magnification satisfies:

$$\sum_i \mathfrak{M}_i = \frac{b_{n-1}}{a_n}. \quad (16)$$

For all of the caustic singularities appearing in the infinite family of A_n ($n \geq 2$), D_n ($n \geq 4$), E_6 , E_7 , E_8 singularities, the coefficient b_{n-1} was shown to be zero, and Theorem 16 was thereby proved. We will illustrate the method of proof here in the case of the hyperbolic umbilic. See [2,3] for a detailed treatment.

The induced map \mathbf{f}_c corresponding to the hyperbolic umbilic is given by:

$$\mathbf{f}_c(x_1, x_2) = (-3x_1^2 - cx_2, -3x_2^2 - cx_1).$$

Let $\mathbf{s} = (s_1, s_2)$ be a target point lying in the four-image region. The four lensed images of \mathbf{s} are obtained by solving for the equation

$$(-3x_1^2 - cx_2, -3x_2^2 - cx_1) = (s_1, s_2). \quad (17)$$

To use the Euler trace formula in the form (16), we begin by eliminating x_2 to obtain a polynomial in the variable x_1 :

$$\varphi(x_1) \equiv -3s_1^2 - c^2s_2 - c^3x_1 - 18s_1x_1^2 - 27x_1^4.$$

The magnification of a lensed image of \mathbf{s} under \mathbf{f}_c is $\mathfrak{M}(x_1, x_2) = 1/(-c^2 + 36x_1x_2)$. To convert this into a rational function in the single variable x_1 , we substitute for x_2 via (17) to obtain:

$$\mathfrak{M}(x_1, x_2(x_1)) = \frac{c}{-c^3 - 36s_1x_1 - 108x_1^3} \equiv \mathfrak{M}(x_1).$$

A direct calculation now yields:

$$\varphi'(x_1)\mathfrak{M}(x_1) = c.$$

Thus the unique polynomial representative in the coset $\overline{\varphi'(x_1)\mathfrak{M}(x_1)}$ is the polynomial $r(x_1) \equiv c$ (in the notation of Theorem 17, $\mathfrak{M}(x_1) \equiv h(x_1)$). Since $b_{n-1} = b_3 = 0$, (16) tells us immediately that

$$\mathfrak{M}_1 + \mathfrak{M}_2 + \mathfrak{M}_3 + \mathfrak{M}_4 = 0.$$

Acknowledgements AOP and MCW would like to thank Amir Aazami and Alberto Tegua for stimulating discussions, and Stanley Absher for editorial assistance.

References

1. Aazami, A. B., Petters, A. O.: A universal magnification theorem for higher-order caustic singularities. *J. Math. Phys.* **50**, 032501, (2009).
2. Aazami, A. B., Petters, A. O.: A universal magnification theorem II. Generic caustics up to codimension five. *J. Math. Phys.* **50**, 082501, (2009).
3. Aazami, A. B., Petters, A. O.: A universal magnification theorem III. Caustics beyond codimension five, to appear in *J. Math. Phys.* (2009), math-ph/0909.5235.
4. Abramowicz, M. A., Carter, B., Lasota, J. P.: Optical reference geometry for stationary and static dynamics. *Gen. Rel. Grav.* **20**, 1173, (1988).
5. Adler R., Taylor J.: *Random Fields and Geometry*. Wiley, London (1981).
6. Arnold, V. I.: Normal forms for functions near degenerate critical points, the Weyl groups of A_k, D_k, E_k and Lagrangian singularities. *Func. Anal. Appl.* **6**, 254, (1973).
7. Arnold, V. I.: Evolution of singularities of potential flows in collision-free media and the metamorphoses of caustics in three-dimensional space. *J. Sov. Math.* **32**, 229, (1986).
8. Arnold, V. I., Gusein-Zade, S. M., and Varchenko, A. N.: *Singularities of Differentiable Maps*, vol. I. Birkhäuser, Boston (1985).
9. Arnold, V. I., Gusein-Zade, S. M., Varchenko, A. N.: *Singularities of Differentiable Maps*, vol. II. Birkhäuser, Boston (1985).
10. Atiyah, M. F., Bott, R.: A Lefschetz fixed point formula for elliptic complexes: I. *Ann. Math.* **86**, 374 (1967).
11. Atiyah, M. F., Bott, R.: A Lefschetz fixed point formula for elliptic complexes: II. Applications. *Ann. Math.* **88**, 451 (1968).
12. Azais J. M., Wschebor M.: On the distribution of the maximum of a Gaussian field with d parameters. *Ann. Appl. Probab.* **15(1A)**, 254 (2005).
13. Bayer, J., Dyer, C.C.: Maximal lensing: mass constraints on point lens configurations. *Gen. Rel. Grav.* **39**, 1413, (2007).
14. Blandford, R. D.: Gravitational lenses. *Q. J. Roy. Astron. Soc.* **31**, 305, (1990).
15. Blandford, R., Narayan, R.: Fermat's principle, caustics, and the classification of gravitational lens images. *Astrophys. J.* **310**, 568, (1986).
16. Burke, W.: Multiple gravitational imaging by distributed masses. *Astrophys. J. Lett.* **244**, L1, (1981).
17. Castrigiano, D., Hayes, S.: *Catastrophe Theory*. Addison-Wesley, Reading (2004).
18. Chiba, M.: Probing dark matter substructure in lens galaxies. *Astrophys. J.* **565**, 17, (2002).
19. Dalal, N.: The magnification invariant of simple galaxy lens models. *Astrophys. J.* **509**, 13, (1998).
20. Dalal, N., Rabin, J. M.: Magnification relations in gravitational lensing via multidimensional residue integrals. *J. Math. Phys.* **42**, 1818, (2001).
21. Evans, N. W., Hunter, C.: Lensing properties of cored galaxy models. *Astrophys. J.* **575**, 68, (2002).
22. Evans, N.W., Witt., H. J.: Are there sextuplet and octuplet image systems? *Mon. Not. Roy. Astron. Soc.* **327**, 1260, (2001).
23. Frankel, T.: *Gravitational Curvature: An Introduction to Einstein's Theory*. W. H. Freeman, San Francisco, CA (1979).
24. Friedrich, H., Stewart, J. M.: Characteristic initial data and wavefront singularities in general relativity. *Proc. R. Soc. Lond. A* **385**, 345(1983).
25. Forrester P. J., Honner, G.: Exact statistical properties of the zeros of complex random polynomials, *J. Phys. A: Math. Gen.* **32**, 2961, (1999).
26. Giannoni, F., Lombardi, M.: Gravitational lenses: odd or even images? *Class. Quantum Grav.* **16**, 1 (1999).
27. Giannoni, F., Masiello, A., Piccione, P.: A Morse theory for light rays on stably causal Lorentzian manifolds. *Ann. Inst. H. Poincaré, Physique Theoretique* **69**, 359 (1998).
28. Gibbons, G. W.: No glory in cosmic string theory. *Phys. Lett. B* **308**, 237, (1993).
29. Gibbons, G. W., Herdeiro, C. A. R., Warnick, C., Werner, M. C.: Stationary metrics and optical Zermelo-Randers-Finsler geometry. *Phys. Rev. D* **79**, 044022, (2009).

30. Gibbons, G. W., Warnick, C. M.: Universal properties of the near-horizon optical geometry. *Phys. Rev. D* **79**, 064031, (2009).
31. Gibbons, G. W., Werner, M. C.: Applications of the Gauss-Bonnet theorem to gravitational lensing. *Class. Quantum Grav.* **25**, 235009, (2008).
32. Gilmore, R.: *Catastrophe Theory for Scientists and Engineers*, Dover (1981).
33. Golubitsky, M., Guillemin, V.: *Stable Mappings and Their Singularities*. Springer, Berlin (1973).
34. Gottlieb, D. H.: A gravitational lens need not produce an odd number of images. *J. Math. Phys.* **35**, 5507, (1994).
35. Granot, J., Schrecker, P. L., Wambsganss, J.: The mean number of extra microimage pairs for macrolensed quasars. *Astrophys. J.* **583**, 575, (2003).
36. Griffiths, P., Harris, J.: *Principles of Algebraic Geometry*. J. Wiley, New York (1994).
37. Hunter, C., Evans, N. W.: Lensing properties of scale-free galaxies. *Astrophys. J.* **554**, 1227, (2001).
38. Katz, N., Balbus, S., Paczyński, B.: Random scattering approach to gravitational microlensing. *Ap. J.* **306**, 2, (1986).
39. Keeton, C. R.: Gravitational lensing with stochastic substructure: Effects of the clump mass function and spatial distribution. <http://xxx.lanl.gov/abs/0908.3001> (2009).
40. Keeton, C., Gaudi, S., Petters, A. O.: Identifying lenses with small-scale structure. I. Cusp lenses. *Astrophys. J.* **598**, 138, (2003).
41. Keeton, C., Gaudi, S., Petters, A. O.: Identifying lenses with small-scale structure. II. Fold lenses. *Astrophys. J.* **635**, 35, (2005).
42. Khavinson, D., Neumann, G.: On the number of zeros of certain rational harmonic functions. *Proc. Amer. Math. Soc.* **134**, 1077, (2006).
43. Kovner, I.: Fermat principle in arbitrary gravitational fields. *Astrophys. J.* **351**, 114, (1990).
44. Li, W.V., Wei, A.: On the expected number of zeros of random harmonic polynomials. *Proc of the A.M.S.* **137**, 195, (2009).
45. Majthay, A.: *Foundations of Catastrophe Theory*. Pitman, Boston (1985).
46. Mao, S., Petters, A. O., Witt, H.: Properties of point masses on a regular polygon and the problem of maximum number of images. In: *Proceedings of the Eighth Marcel Grossman Meeting on General Relativity*, Ed. T. Piran, World Scientific, Singapore (1997).
47. Mao, S., Schneider, P.: Evidence for substructure in lens galaxies? *Mon. Not. Roy. Astron. Soc.* **295**, 587, (1998).
48. McKenzie, R. H.: A gravitational lens produces an odd number of images. *J. Math. Phys.* **26**, 1592, (1985).
49. Metcalf, R. B., Madau, P.: Compound gravitational lensing as a probe of dark matter substructure within galaxy halos. *Astrophys. J.* **563**, 9, (2001)
50. Milnor, J.: *Dynamics in One Complex Variable*. Princeton University Press, Princeton (2006).
51. Narasimha, D., Subramanian, K.: ‘Missing image’ in gravitational lens systems? *Nature* **310**, 112, (1986).
52. Nityananda, R., Ostriker, J. P.: Gravitational lensing by stars in a galaxy halo - Theory of combined weak and strong scattering. *J. Astrophys. Astr.* **5**, 235, (1984).
53. Orban de Xivry, G., Marshall, P.: An atlas of predicted exotic gravitational lenses. astro-ph/0904.1454 (2009)
54. Padmanabhan, T., Subramanian, K.: The focusing equation, caustics and the condition for multiple imaging by thick gravitational lenses. *Mon. Not. R. Astron. Soc.* **233**, 265, (1988).
55. Perlick, V.: On Fermat’s principle in general relativity: I. The general case. *Class. Quantum Grav.* **7**, 1319, (1990).
56. Perlick, V.: On Fermat’s principle in general relativity: II. The conformally stationary case. *Class. Quantum Grav.* **7**, 1849 (1990)
57. Perlick, V.: Infinite dimensional Morse theory and Fermat’s principle in general relativity I. *J. Math. Phys.* **36**, 6915, (1995).
58. Perlick, V.: Criteria for multiple imaging in Lorentzian manifolds. *Class. Quantum Grav.* **13**, 529, (1996).
59. Perlick, V.: Global properties of gravitational lens maps in a Lorentzian manifold setting. *Commun. Math. Phys.* **220**, 403–428 (2001)
60. Perlick, V.: *Ray Optics, Fermat’s Principle, and Applications to General Relativity*. Springer-Verlag, Berlin (2000).
61. Petters, A. O.: Singularities in gravitational microlensing. Ph.D. Thesis, MIT, Department of Mathematics, (1991);
Petters, A. O.: Morse theory and gravitational microlensing. *J. Math. Phys.* **33**, 1915, (1992);
Petters, A. O.: Multiplane gravitational lensing. I. Morse theory and image counting. *J. Math. Phys.* **36**, 4263, (1995).
62. Petters, A. O.: Arnold’s singularity theory and gravitational lensing. *J. Math. Phys.* **33**, 3555, (1993).
63. Petters, A. O.: Multiplane gravitational lensing III: Upper bound on number of images. *J. Math. Phys.* **38**, 1605, (1997).
64. Petters, A. O., Levine, H., Wambsganss, J.: *Singularity Theory and Gravitational Lensing*. Birkäuser, Boston (2001).
65. Petters, A. O., Rider, B., Teguiä, A. M.: A mathematical theory of stochastic microlensing I. Random time delay functions and lensing maps. *J. Math. Phys.* **50**, 072503 (2009).
66. Petters, A. O., Rider, B., Teguiä, A. M.: A mathematical theory of stochastic microlensing II. Random images, shear, and the Kac-Rice formula, to appear in *J. Math. Phys.* (2009), astro-ph/0807.4984v2.
67. Petters, A. O., Wicklin, F. W.: Fixed points due to gravitational lenses. *J. Math. Phys.* **39**, 1011 (1998)
68. Poston, T., Stewart, I.: *Catastrophe Theory and its Applications*. Dover, New York (1978).
69. Rhie, S. H.: Infimum microlensing amplification of the maximum number of images of n-point lens systems. *Astrophys. J.* **484**, 67 (1997).
70. Rhie, S. H.: n-point gravitational lenses with $5(n - 1)$ images. astro-ph/0305166 (2003).
71. Renn, J., Sauer, T., Stachel, J.: The origin of gravitational lensing: a postscript to Einstein’s 1936 *Science Paper*. *Science* **275**, 184 (1997).
72. Schneider, P., Ehlers, J., Falco, E. E.: *Gravitational Lenses*. Springer, Berlin (1992).
73. Schneider, P., Weiss, A.: The two-point mass lens: detailed investigation of a special asymmetric gravitational lens. *Astron. Astrophys.* **164**, 237 (1986).

74. Schneider, P., Weiss, A.: The gravitational lens equation near cusps. *Astron. Astrophys.* **260**, 1, (1992).
75. Shin, E. M., Evans, N. W.: The Milky Way Galaxy as a strong gravitational lens. *Mon. Not. Roy. Astron. Soc.* **374**, 1427, (2007).
76. Shub, M., Smale, S.: *Complexity of Bezout's theorem. II. Volumes and Probabilities, Computational Algebraic Geometry, Nice (1992), Progress in Mathematics* vol. 109. Birkhäuser, Boston (1993).
77. Sodin, M., Tsirelson, B.: Random complex zeroes, I. Asymptotic normality. *Israel Journal of Mathematics* **144**, 125 (2004);
Sodin, M., Tsirelson, B.: Random complex zeroes, II. Perturbed lattice. *Israel Journal of Mathematics* **152**, 105 (2006);
Sodin, M., Tsirelson, B.: Random complex zeroes, III. Decay of the hole probability. *Israel Journal of Mathematics* **147**, 371 (2005).
78. Subramanian, K., Cowling, S.: On local conditions for multiple imaging by bounded, smooth gravitational lenses. *Mon. Not. R. astr. Soc.* **219**, 333 (1986).
79. Wambsganss, J., Witt, H.J., Schneider, P.: Gravitational microlensing - powerful combination of ray-shooting and parametric representation of caustics. *Astron. Astrophys.* **258**, 591 (1992).
80. Werner, M. C.: A Lefschetz fixed point theorem in gravitational lensing. *J. Math. Phys.* **48**, 052501 (2007).
81. Werner, M. C.: Geometry of universal magnification invariants. *J. Math. Phys.* **50**, 082504 (2009).
82. Witt, H.: Investigation of high amplification events in light curves of gravitationally lensed quasars. *Astron. Astrophys.* **236**, 311 (1990).
83. Witt, H. J., Mao, S.: On the minimum magnification between caustic crossings for microlensing by binary and multiple Stars. *Astrophys. J. Lett.* **447**, 105, (1995).
84. Witt, H. J., Mao, S.: On the magnification relations in quadruple lenses: a moment approach. *Mon. Not. Roy. Astron. Soc.* **311**, 689, (2000).
85. Zakharov, A.: On the magnification of gravitational lens images near cusps. *Astron. Astrophys.* **293**, 1 (1995).